Available online at www.sciencedirect.com
SCIENCE DIRECT®
Journal of Theoretical Biology 227 (2004) 463–486
Journal of Theoretical Biology
www.elsevier.com/locate/jtbi

The human immune response to *Mycobacterium tuberculosis* in lung and lymph node

Simeone Marino*, Denise E. Kirschner

Department of Microbiology and Immunology, University of Michigan Medical School, 6730 Medical Science Building II, Ann Arbor, MI 48109-0620, USA

Received 12 August 2003; received in revised form 6 November 2003; accepted 17 November 2003

Abstract

A key issue for the study of tuberculosis is to understand why individuals infected with *Mycobacterium tuberculosis* (*Mtb*) experience different clinical outcomes. To better understand the dynamics of *Mtb* infection and immunity, we have previously developed a temporal mathematical model that qualitatively and quantitatively characterizes the cellular and cytokine control network during infection. In this work we extend that model to a two compartmental model to capture the important processes of cellular activation and priming that occur between the lung and the nearest draining lymph node. We are able to reproduce typical disease progression scenarios including primary infection, latency or clearance. Then we use the model to predict key processes determining these different disease trajectories (i.e. identify bifurcation parameters), suggesting directions for further basic science study and potential new treatment strategies.

Keywords: Human; *M. tuberculosis*; Lung and lymph nodes; Model; Dendritic cells

1. Introduction

Mycobacterium tuberculosis (*Mtb*) is a facultative intracellular pathogen that has infected almost one-third of the world population. Although the majority (about 90%) of infected individuals mount a protective and effective cell-mediated response and do not develop active disease, tuberculosis (TB) is still one of the major causes of death by infectious disease worldwide with more than 3 million deaths per year (Abu-Amero, 2002; Dye et al., 1999). Most individuals infected with *Mtb* are able to control infection (not clear it) and settle into a latent state. Others develop active disease in either short term (primary infection) or long term (reactivation). What distinguishes these different infection outcomes is unclear and it is the motivation for this work.

TB disease progression is relatively slow compared to many other bacterial and viral infections: *M. tuberculosis* doubles approximatively every 18–48 h, while some pathogen have doubling times on the order of minutes. A typical primary TB progression may have a time course ranging from 1 to 5 years with reactivation an even longer process, up to at least 33 years (Arend and van Dissel, 2002; Lillebaek et al., 2002). Nevertheless, what happens in the early stages of the host–pathogen interaction is likely relevant to understanding different infection outcomes.

M. tuberculosis dynamics within the host most often occurs in the respiratory tract: the majority of patients who develop TB have symptoms that are restricted to the lung (pulmonary TB). During infection, macrophages represent both victims and heroes. They are the prime target cells; however, after their activation they can kill intracellular bacteria and participate in a protective T helper cell type 1 (Th1) response (Th2 response targets extracellular bacteria and is called humoral immunity).

In mycobacterial infection, Th1-type cytokines have been shown to be essential for protective immunity (Flynn and Chan, 2001). Both CD4+ and CD8+ T cells provide protection against *M. tuberculosis* (Caruso et al., 1999; Tascon et al., 1998); however, T-cell effector function can be achieved only after priming and

*Corresponding author. Tel.: +1-734-647-7722; fax: +1-734-647-7723.
E-mail addresses: simeonem@umich.edu (S. Marino), kirschne@umich.edu (D.E. Kirschner).

0022-5193/$ - see front matter © 2003 Elsevier Ltd. All rights reserved.
doi:10.1016/j.jtbi.2003.11.023

differentiation occur. While T cell priming is thought to occur primarily in the draining lymph nodes (DLNs) of the lung, Th1/Th2 differentiation is still far from understood (Allen and Maizels, 1997; Annunziato et al., 1998; Bottomly, 1999; Janeway, 2001; Lanzavecchia and Sallusto, 2000; Romagnani et al., 1998; Romagnani, 1998, 1999, 2000; Rook, 2001). Not only is the location of differentiation still controversial, but what determines final T helper cell fate is not yet clear, likely involving multiple factors. There is also a bi-potential stage in T helper cell differentiation, namely Th precursor (Th_P), Th0 or non-polarized helper T cells (Lanzavecchia and Sallusto, 2000; Sallusto et al., 1999; Sallusto and Lanzavecchia, 2000; Sallusto et al., 2000). While Th_P can be stimulated to produce both Th1-type and Th2-type cytokines, Th1 and Th2 are likely already committed. The existence of Th precursors is controversial, and indeed this class may encompass a spectrum of cells differentiating from naïve to Th1/Th2 phenotypes, as well as memory T cells (Lanzavecchia and Sallusto, 2000; Langenkamp et al., 2000).

The immune response to Mtb infection is unique in the formation of spherical structures known as granulomas. Because our efforts are to study human TB and little to no information is available regarding granuloma formation and function in humans, we rely on the sole measurement source of data from humans: that of bronco-alveolar lavage (BAL) fluid. It is fluid drawn from the lung that provides a rough indicator of the cells and cytokines present in the lung. Therefore, in this study, we focus exclusively on temporal dynamics. In other work we are exploring the intricate spatial details of granuloma formation using a number of formulations (Gammack et al., 2003).[1]

There is growing evidence that information needed to generate different types of immune responses is controlled by dendritic cells (DCs), the most efficient antigen presenting cells (Bottomly, 1999; Lanzavecchia and Sallusto, 2000). While mycobacteria–macrophage interactions have been extensively addressed (Flynn and Chan, 2001), recent studies have focused on the interaction of *M. tuberculosis* with DCs (Bodnar et al., 2001; Demangel and Britton, 2000; Feng et al., 2001; Giacomini et al., 2001; Hickman et al., 2002; Jiao et al., 2002).

Immature or resting DCs (IDC) are highly represented at sites of *M. tuberculosis* infection (such as the lung) at the onset of the inflammatory response (Banchereau and Steinman, 1998; Banchereau et al., 2000; Gonzalez-Juarrero and Orme, 2001; Guermonprez et al., 2002; Holt and Schon-Hegrad, 1987; Holt et al., 1993; Holt, 2000; Sertl et al., 1986; van Haarst et al., 1994): they are specialized for antigen uptake and processing (Giacomini et al., 2001; Hickman et al., 2002; Banchereau and Steinman, 1998; Banchereau et al., 2000; Guermonprez et al., 2002; Havenith et al., 1992; Henderson et al., 1997). Following microbial encounter and internalization, IDCs undergo maturation (Mature DCs, MDCs), as observed both *in vitro* and *in vivo* (Banchereau et al., 2000) and migrate to secondary lymphoid tissues. The maturation-migration process of DCs to the DLN is enhanced during *M. tuberculosis* infection, while, on the contrary, infected macrophages show little phenotypic change (Flynn and Chan, 2001; Giacomini et al., 2001; Hickman et al., 2002; DesJardin et al., 2002). This is confirmed by recent studies highlighting how, after *M. tuberculosis* infection, MDCs release Th1-inducing cytokines (IL-12 and IFN-α) in very consistent amounts (Giacomini et al., 2001; Hickman et al., 2002; Gonzalez-Juarrero and Orme, 2001). On the contrary, infected macrophages produce mainly proinflammatory cytokines (IL-10, TNF-α) (Giacomini et al., 2001; Hickman et al., 2002). Thus, during *M. tuberculosis* infection, macrophages and DCs likely play different roles: macrophages secrete proinflammatory cytokines inducing an inflammatory response, whereas DCs are primarily involved in inducing anti-mycobacterial T-cell mediated immunity. As MDCs are known to migrate to the DLN for presentation to naïve T cells, it seems likely that a default Th1-type environment is present in the DLN during the infection process (Russo et al., 2000), beginning from early stage of infection (Langenkamp et al., 2000). The cytokine environment in the lung (GM-CSF, IL-10 and IL-4) may also play a role in monocyte maturation (Fortsch et al., 2000), defining cell population phenotypes at the site of infection (Palucka et al., 1998).

To address some of the questions, hypothesis and theories outlined above, we develop and analyse a mathematical model of *M. tuberculosis* infection. We use a 2-compartmental model which is needed to capture the relevant migration patterns between DLN and lung. Our goal is to test our model by simulating different infection outcomes in humans during *M. tuberculosis* infection and then use the model to predict key processes determining these different infection outcomes (i.e. identify bifurcation parameters). Throughout we compare our results with known or generated experimental data.

2. Mathematical model

A minimum of two compartments is relevant when modeling this complex immunoregulatory system: the site of infection (lung) and the peripheral DLN (Hilar

[1] S. Ganguli et al. (submitted, September 2003), Metapopulation model of granuloma formation in the lung during *Mycobacterium tuberculosis* infection.

Jose L. Segovia-Juarez, Suman Ganguli, Denise E. Kirschner (to be submitted), An Agent Base Model of Granuloma Formation in *Mycobacterium tuberculosis* infection.

region). Building on an existing virtual model of the host response to *M. tuberculosis* (Wigginton and Kirschner, 2001) referred to as the "lung model", we address DLN dynamics and compare them with that occurring in the infected lung.

2.1. Lung compartment

The lung model that we previously developed (Wigginton and Kirschner, 2001) describes what occurs at the site of infection, with particular emphasis on macrophage and lymphocyte interactions with *M. tuberculosis*. To extend this model to consider the importance of the lymph nodes as the priming location, we must then address the role of DCs, which were not previously included in the model.

Within the lung the relevant cell-types present are macrophages (resting-M_R, activated-M_A and infected-M_I), bacteria (both extracellular-B_E and intracellular-B_I) and lymphocytes (Th_P, Th1 and Th2). In this model we do not consider effector CD8+T cells (CTLs) directly, but we include their effects indirectly (see below). In other work we explore the role of CTLs in *Mtb* infection in a more mechanistic fashion.[2]

We also include four cytokines in this model as we have previously (Wigginton and Kirschner, 2001): IFN-γ, IL-12, IL-4 and IL-10. These four cytokines have been shown to be correlated with infection dynamics (Flynn et al., 1993; Newport et al., 1996; Fulton et al., 1998; Isler et al., 1999; Moore et al., 2001; Flynn and Chan, 2001, p. 105). One other, TNF-α, has recently been observed to have both chemotactic and anti- and pro-inflammatory effects. We also study the unique role of TNF-α in other work.[3]

The two-compartmental model includes five new variables, and consequently five new equations, in order to implement the hypotheses discussed above. The five new model variables may be divided into four that are operating in the DLN and one acting in the lung. To avoid confusion, Th precursors and IL-12 in the DLN will be denoted as Th_P^{LN} and I_{12}^{LN}, respectively. T represents naïve T cells and IDC and MDC, immature and mature dendritic cells, respectively (see Table 1).

2.1.1. Macrophages

Macrophage populations (M_R, M_A and M_I) are described in Eqs. (1.1)–(1.3). Resting or resident macrophages (M_R) are normally present in the lung (Antony et al., 1993; Condos et al., 1998; Law et al., 1996; Schwander et al., 1998). Macrophages have a natural turnover, a source (s_M) of new cells coming into the site (due to monocytes differentiation) and natural death (half-life) of cells (at rate μ_R). Without infection, the macrophage population should remain at the equilibrium value, $\bar{M}_R = s_M/\mu_R$. During infection, resident macrophages undergo three different dynamics: enhanced recruitment, infection and activation. Recruitment is triggered via a chemokine gradient by bacterial invasion, expressed by the total number of bacteria at the site of infection ($B_T = B_I + B_E$), that also contributes to infection of resident macrophages and their activation (together with IFN-γ). When bacteria are present, additional resting macrophages are recruited to the site of infection in the lung in response to chemokines released by activated and infected macrophages, at rates α_4 and $w\alpha_4$, respectively (with $0<w<1$, with the action of activated likely stronger than that of infected).

While bacteria are sufficient for infection, IFN-γ is required for macrophage activation (Flesch and Kaufmann, 1990; Nathan et al., 1983; Stout and Bottomly, 1989), occurring at a maximum rate of k_3. The cytokine environment affects the regulation of the immune response at the site of infection, slowing down macrophage activation under the action of IL-4 (Maggi et al., 1992; Szabo et al., 1997) and facilitating macrophage deactivation (IL-10 downregulation), at maximal rate k_4. Activated macrophages undergo natural death (at rate μ_A).

Resting macrophages that are unable to clear their bacterial load may become chronically infected (Janeway, 2001; McDonough et al., 1993; Sturgill-Koszycki et al., 1994), at maximal rate k_2. Chronic infection results in either infected macrophage killing or natural death (at rate μ_I). Killing is enhanced by intracellular bacteria proliferation (and subsequent infected macrophage bursting), at maximal rate k_{17}. Both apoptosis and cytotoxic activity are due to CD4+ or Th1 cells (by Fas-FasL) and to CD8+ or CTL cells (by granzyme and perforin) (Lalvani et al., 1998; Lewinsohn et al., 1998; Oddo et al., 1998; Skinner et al., 1997; Tan et al., 1997; Tsukaguchi et al., 1995).

Assuming that the average maximal bacterial carrying capacity per macrophage (or the multiplicity of infection, MOI) is N, intracellular bacterial proliferating beyond this threshold results in bursting of M_I and subsequent release of their intracellular bacterial load. *M. tuberculosis* might have the capacity to control T-cell mediated lysis of its host macrophage, either by down-regulating receptor expression on the macrophage (blocking the STAT-1 induced transcription) or by other unknown mechanisms (Balcewicz-Sablinska et al., 1998; Keane et al., 2000; Rojas et al., 1999).

Since in this model CTLs are not included directly, we consider the action of CTLs proportional to Th1-effector function (targeting intracellular bacteria), thus the effector cell to target cell ratio ($Th1/M_I$) indirectly

[2] Dhruv Sud and Denise Kirschner (submitted Jan 2004), The role of TNF-α and CD8+ T cells in controlling *Mycobacterium tuberculosis* infection.

[3] Ibidem

Table 1
Comparison of the variables of the lung model (Wigginton and Kirschner, 2001) and of the new two-compartmental model. In bold are new variables

Variables	Lung model	New two-compartmental model	
		Lung	Lymph node
Macrophages	Resting, activated and infected	Resting, activated and infected	—
Dendritic cells	—	**Immature DC**	**Mature DC**
Lymphocytes	Th0, Th1 and Th2	Th0, Th1 and Th2	**Naïve T cells and Th0**
Bacteria	Intracellular and extracellular	Intracellular and extracellular	—
Cytokines	IL-12, IFN-γ, IL-4, IL-10	IL-12, IFN-γ, IL-4, IL-10	**IL-12**

determines the rate of M_I killing (with a maximum at k_{14}), and is half-maximal when this ratio is equal to c_4 (Eq. (1.3)).

recruitment infection

$$\frac{dM_R}{dt} = s_M + \alpha_4(M_A + wM_I) - k_2 M_R\left(\frac{B_E}{B_E + c_9}\right) + k_4 M_A\left(\frac{I_{10}}{I_{10} + sc_8}\right) - k_3 M_R\left(\frac{I_\gamma}{I_\gamma + f_3 I_4 + sc_3}\right)\left(\frac{B_T}{B_T + c_8}\right) - \mu_R M_R$$

activation death de-activation death

(1.1)

$$\frac{dM_A}{dt} = k_3 M_R\left(\frac{I_\gamma}{I_\gamma + f_3 I_4 + sc_3}\right)\left(\frac{B_T}{B_T + c_8}\right) - k_4 M_A\left(\frac{I_{10}}{I_{10} + sc_8}\right) - \mu_A M_A \quad (1.2)$$

$$\frac{dM_I}{dt} = k_2 M_R\left(\frac{B_E}{B_E + c_9}\right) - k_{17} M_I\left(\frac{B_I^m}{B_I^m + (NM_I)^m}\right) - k_{14} M_I\left(\frac{\frac{T_1}{M_I}}{\frac{T_1}{M_I} + c_4}\right) - \mu_I M_I$$

infection bursting MI killing by cell-mediated immunity death

(1.3)

2.1.2. Cytokines

Cytokines are produced by a large variety of cells involved both in the innate and adaptive immunity (Lucey et al., 1996). We consider direct cytokine production by macrophages and lymphocytes and an extra source of IFN-γ (from CD8+ T cells) (Lazarevic and Flynn, 2002; Serbina and Flynn, 1999, 2001). Four concentrations are described representing respectively two key Type I cytokines (IFN-γ and IL-12, Eqs. (1.4) and (1.5), respectively), and two Type II (or anti-Type I-inducing) cytokines (IL-10 and IL-4, Eqs. (1.6) and (1.7), respectively).

IFN-γ gene knockout (KO) mice are highly susceptible to *M. tuberculosis* (Cooper et al., 1993) and individuals lacking receptors for IFN-γ suffer from recurrent, sometimes lethal mycobacterial infections (Flynn et al., 1993; Newport et al., 1996). Th2-type cytokines inhibit the *in vitro* production of IFN-γ (Lucey et al., 1996; Powrie and Coffman, 1993), as well as macrophage activation (Appelberg et al., 1992), and may therefore weaken host defense (de Waal Malefyt et al., 1993). IFN-γ is mainly produced by Th1 cells, before and after activated macrophage action (at rate α_5) (Barnes et al., 1993; Fulton et al., 1998; Tsukaguchi et al., 1999). An additional source of this cytokine is included in the model (s_g) since CD8+ T cells have been shown to be a potent producer (Lazarevic and Flynn, 2002; Serbina and Flynn, 1999). This source is a function of the bacterial concentration and IL-12, implying that the degree of infection and IL-12 concentration represents the level of CTL immunity present (Cooper et al., 1997; Wakeham et al., 1998). IFN-γ decays at rate μ_g (Kurzrock et al., 1985).

IFN-γ production by other souces (NK, CD8,..), induced by IL-12 and B_T — **IFN-γ** production by Th1, induced by M_A — death

$$\frac{dI_\gamma}{dt} = s_g\left(\frac{B_T}{B_T + c_{10}}\right)\left(\frac{I_{12}^L}{I_{12}^L + sc_4}\right) + \alpha_5 T_1\left(\frac{M_A}{M_A + c_5}\right) - \mu_g I_\gamma \quad (1.4)$$

IL-12 production by M_A and M_R — death

$$\frac{dI_{12}^L}{dt} = \alpha_8 M_A + \alpha_{23} M_R - \mu_{I_{12}^L} I_{12}^L \quad (1.5)$$

IL-10 production by M_A, opposed by IFN-g and IL-10 — **IL-10** production by Th1, Th2 and ThP — IL-10 production by M_I — death

$$\frac{dI_{10}}{dt} = \alpha_{14} M_A\left(\frac{sc_6}{I_{10} + f_6 I_\gamma + sc_6}\right) + \alpha_{16} T_1 + \alpha_{17} T_2 + \alpha_{18} T_P^L + \delta_7 M_I - \mu_{I_{10}} I_{10} \quad (1.6)$$

IL-4 production by ThP and Th2 — death

$$\frac{dI_4}{dt} = \alpha_{11} T_P^L + \alpha_{12} T_2 - \mu_{I_4} I_4 \quad (1.7)$$

IL-12 in the lung is produced mainly by activated and resident macrophages (at rates α_8 and α_{23}, respectively)

(Chensue et al., 1995; Fulton et al., 1996, 1998; Isler et al., 1999).

Its main effect is to enhance cell-mediated immunity, both directly (enhancing Th precursor differentiation to Th1) (Manetti et al., 1993; O'Garra, 1998; Sornasse et al., 1996) and indirectly (facilitating the production of IFN-γ) (O'Donnell et al., 1999). IL-12 decays at rate $\mu_{I_{12}}$ (Remick and Friedland, 1997). IL-10 is a down regulatory cytokine (Moore et al., 2001). Its action affects both macrophages and lymphocytes and is always opposed by IFN-γ and by IL-10 itself, defining a complex feedback mechanism suppressing cell-mediated immunity. Th1 (at rate α_{16}) and Th2 (at rate α_{17}) cells produce IL-10 (Lucey et al., 1996; Meyaard et al., 1996; Peng et al., 1997; Yssel et al., 1992), as well as Th precursor (at rate α_{18}). Macrophages also secrete this cytokine, especially M_I (at rate δ_7, after *M. tuberculosis* infection). IL-10 decays at rate $\mu_{I_{10}}$ (Huhn et al., 1996, 1997). IL-4 is the key type 2 cytokine, governing Th precursor differentiation to Th2 and down-regulating Th precursor differentiation to Th1 (Maggi et al., 1992; Szabo et al., 1997). It is mainly produced by Th precursor (at rate α_{11}) and Th2 cells (at rate α_{12}). IL-4 decays at rate μ_{I_4} (Remick and Friedland, 1997).

2.1.3. Lymphocytes (Th_P, Th1 and Th2)

The lymphocyte population in the lung is comprised of Th precursor, Th1 and Th2 cells. These three classes of T cells have a finite lifetime and die at rates μ_{T_0}, μ_{T_1} and μ_{T_2}, respectively. Th precursor lymphocytes (Eq. (1.8)), migrating from the draining lymph node through blood vessels (at a maximal rate ξ, induced by chemokine concentrations released by activated macrophages) represent the main source of new Th precursor in the lung (see Eq. (1.15), p. 18). Once in the lung, activated macrophages enhance Th precursor proliferation (at a maximal rate α_2). Th precursor may also differentiate to either Th1 (at a maximal rate k_6) or Th2 (at a maximal rate k_7) and cytokines environment likely drives this differentiation.

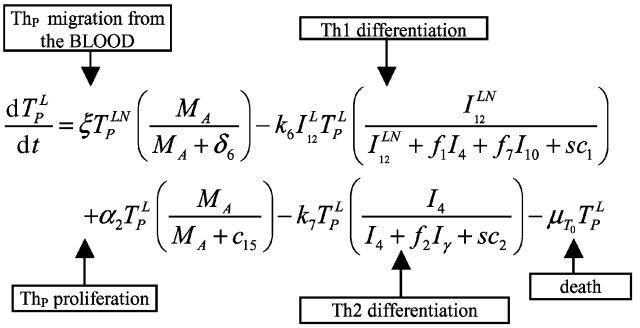

$$\frac{dT_P^L}{dt} = \xi T_P^{LN}\left(\frac{M_A}{M_A+\delta_6}\right) - k_6 I_{12}^L T_P^L\left(\frac{I_{12}^{LN}}{I_{12}^{LN}+f_1 I_4+f_7 I_{10}+sc_1}\right) + \alpha_2 T_P^L\left(\frac{M_A}{M_A+c_{15}}\right) - k_7 T_P^L\left(\frac{I_4}{I_4+f_2 I_\gamma+sc_2}\right) - \mu_{T_0} T_P^L \tag{1.8}$$

$$\frac{dT_1}{dt} = k_6 I_{12}^L T_P^L\left(\frac{I_{12}^{LN}}{I_{12}^{LN}+f_1 I_4+f_7 I_{10}+sc_1}\right) - \mu_{T_1} T_1, \tag{1.9}$$

$$\frac{dT_2}{dt} = k_7 T_P^L\left(\frac{I_4}{I_4+f_2 I_\gamma+sc_2}\right) - \mu_{T_2} T_2. \tag{1.10}$$

Inflammatory (e.g. IL-12^{LN} and IFN-γ) and anti-inflammatory cytokines (e.g. IL-10 and IL-4) form an intricate network facilitating either a dominant Th1 or a Th2 response (Sallusto and Lanzavecchia, 2000; Sallusto et al., 2000, 1998) (Eqs. (1.9) and (1.10), respectively). In particular very early presence of IL-12 in the DLN might have a decisive effect in Th1 differentiation.

2.1.4. Bacterial subpopulations

We define two bacterial subpopulations: intracellular (B_I) and extracellular bacteria (B_E). Intracellular bacteria are those that have been internalized by macrophages and immature DCs, while all other bacteria are considered extracellular. Both subpopulations undergo proliferation. Extracellular bacteria are killed by activated and resident macrophages (at rate k_{15} and k_{18}, respectively) while intracellular are killed only when its infected macrophage is killed via CTL action or apoptosis.

Following Eq. (1.3), the maximal intracellular carrying capacity for the entire population of chronically infected macrophages is given by the product $N*M_I$. The number of bacteria released after macrophages undergo apoptosis is only a fraction ($N_1 < N$) of the carrying capacity (N_1 being the average number of intracellular bacteria).

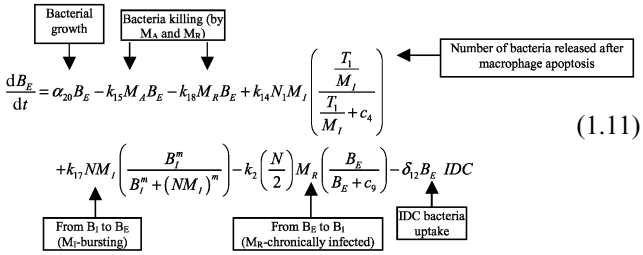

$$\frac{dB_E}{dt} = \alpha_{20}B_E - k_{15}M_A B_E - k_{18}M_R B_E + k_{14}N_1 M_I\left(\frac{\frac{T_1}{M_I}}{\frac{T_1}{M_I}+c_4}\right) + k_{17}NM_I\left(\frac{B_I^m}{B_I^m+(NM_I)^m}\right) - k_2\left(\frac{N}{2}\right)M_R\left(\frac{B_E}{B_E+c_9}\right) - \delta_{12}B_E\ IDC \tag{1.11}$$

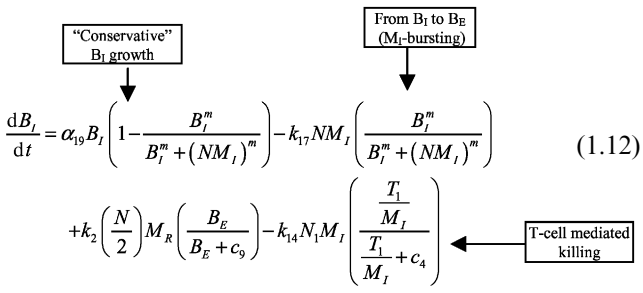

$$\frac{dB_I}{dt} = \alpha_{19}B_I\left(1-\frac{B_I^m}{B_I^m+(NM_I)^m}\right) - k_{17}NM_I\left(\frac{B_I^m}{B_I^m+(NM_I)^m}\right) + k_2\left(\frac{N}{2}\right)M_R\left(\frac{B_E}{B_E+c_9}\right) - k_{14}N_1M_I\left(\frac{\frac{T_1}{M_I}}{\frac{T_1}{M_I}+c_4}\right) \tag{1.12}$$

Exchange of bacteria between extracellular and intracellular compartments due to the natural life spans of chronically infected macrophages is included in this

cytotoxic term. On the contrary, when bursting occurs, the total number of bacteria is released (at a maximal rate of k_{17}). Extracellular bacteria become intracellular when their host macrophage becomes chronically infected.

We assume that such a macrophage carries approximately one-half of its maximal carrying capacity ($N/2$ bacteria), with a maximal rate of bacteria load of $k_2(N/2)$ (as in Eq. (1.1)). Also shown here is the process of immature dendritic cells internalizing extracellular bacteria (at rate δ_{12}).

2.2. Draining lymph node compartment

In order to define the dynamics occurring in the DLN, we make the following assumptions (see Fig. 1; note that the assumptions can easily be modified in the model framework). Antigen presentation activity in the DLN is performed only by MDCs. Only naïve T cells and non-polarized Th cells (Th_P) are present in the DLN. IDCs migrate from the lung to the DLN after they take up bacteria. IDCs internalize bacteria and those bacteria are lost to model the dynamics.

As maturation occurs, DCs migrate through the afferent lymphatic vessels and enter the T cell area of the DLN, where they perform two main functions: naïve T cell recruitment and antigen presentation. In fact, naïve T cell circulation through the DLN is enhanced by chemokines released by MDCs (Janeway, 2001; Zhu et al., 2000), increasing presentation and priming in the T cell area. MDCs also release large amounts of Type I (IL-12) and Type I-inducing cytokines.

Once presentation occurs, naïve T cells experience stages of differentiation, from naïve to effector T cell (von Andrian and MacKay, 2000). The first step, from naïve to Th precursor or non-polarized T cells takes place in the DLN. This phenotypic and functional change allows primed T cells to proliferate and then migrate through the efferent lymphatic vessels into the blood, eventually into the site of infection (von Andrian and MacKay, 2000). During migration and at the site of infection, the cytokine environment drives their final commitment to become effector T cells, i.e. Th1 or Th2. They might also remain in a Th precursor state and then revert to a resting state or become memory T cells (we do not address memory T cell dynamics in the present model).

Our main hypothesis regarding T cell populations is then that the primary output from the DLN is mainly of Th precursor-type that is modulated by the local cytokine environment on the way to, and at the site of infection (Palucka et al., 1998; Rescigno and Borrow, 2001; Rescigno, 2002). A Th1-type response may eventually be initiated directly in the DLN if the amount of Th1-inducing cytokines (IL-12) is considerably large and the number of MDCs present is high (Langenkamp et al., 2000). A strong and sustained Th1 response is not always desirable as it may lead to extensive inflammation and unnecessary tissue damage. In fact, a predominant Th1-response may not always mean disease resolution (Lin et al., 1996; North, 1998) and Th1 differentiation, while necessary, is likely not sufficient (Wigginton and Kirschner, 2001).

2.2.1. IL-12 in the DLN (I_{12}^{LN})

IL-12 in the DLN (Eq. (1.13)) is produced by MDCs (at rate δ_1) and undergoes a natural decay ($-\mu_{I_{12}^{LN}} I_{12}^{LN}$). It drives Th1 differentiation and the amount released in the DLN can affect the final

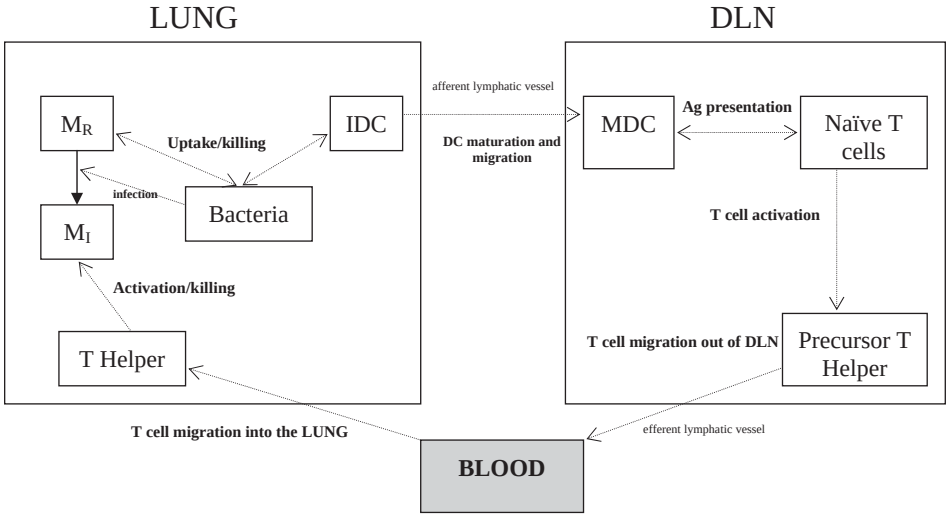

Fig. 1. Scheme representing uptake, trafficking and presentation in *M. tuberculosis* infection.

commitment of T cells in the lung (see Eq. (1.8), Th precursor differentiation to Th1).

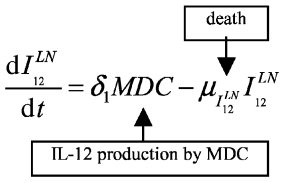

$$\frac{dI_{12}^{LN}}{dt} = \delta_1 MDC - \mu_{I_{12}^{LN}} I_{12}^{LN} \tag{1.13}$$

2.2.2. Naïve T cell (T)

Naïve T cells (Eq. (1.14)) continuously recirculate through the DLN and the blood, with a constant amount migrating in (s_T) and a variable amount (proportional to how many are present; Janeway, 2001) migrating out ($\lambda_1 T$), depending on the number of successful MDC presentations (Lanzavecchia et al., 2001a, b). Their recruitment is also enhanced at a rate (δ_2) proportional to the number of MDCs. They differentiate into Th precursor cells after MDC presentation ($-\delta_4 TMDC$), giving a loss term in Eq. (1.14) and a gain term in Eq. (1.15). They finally undergo natural death (at rate μ_T) (Holt, 2000; Holt and Stumbles, 2000a, b).

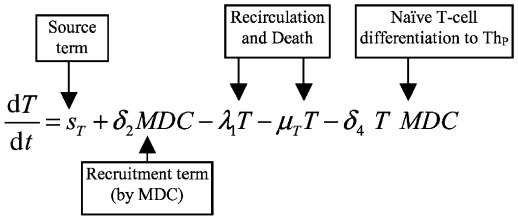

$$\frac{dT}{dt} = s_T + \delta_2 MDC - \lambda_1 T - \mu_T T - \delta_4\, T\, MDC \tag{1.14}$$

2.2.3. Th_P in the DLN (T_P^{LN})

Th precursor cells in the DLN (Eq. (1.15)) undergo proliferation and migration to the lung. Proliferation and death is expressed by a logistic growth rate (with a maximal T_P^{LN} carrying capacity of ρ). A percentage (ξ) of T_P^{LN} cells migrate into the blood and eventually enter the site of infection (Lanzavecchia and Sallusto, 2000).

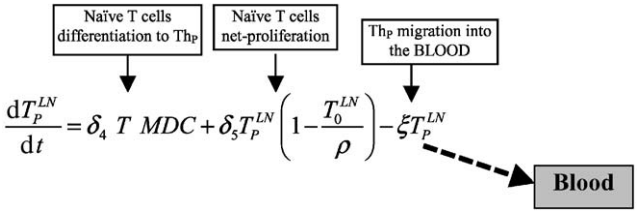

$$\frac{dT_P^{LN}}{dt} = \delta_4\, T\, MDC + \delta_5 T_P^{LN}\left(1 - \frac{T_0^{LN}}{\rho}\right) - \xi T_P^{LN} \tag{1.15}$$

2.2.4. Mature DC in the DLN (MDC)

MDC population dynamics in the DLN (Eq. (1.16)) are determined by IDC maturation and migration from the lung (at a maximal rate δ_{10}), after phagocytosis. They also undergo a natural death (μ_{MDC}) which might account for MDC "deactivation" (exhaustion) (Lanzavecchia and Sallusto, 2001a, b).

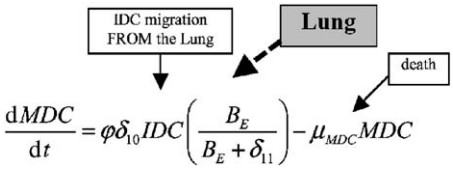

$$\frac{dMDC}{dt} = \varphi\delta_{10} IDC\left(\frac{B_E}{B_E + \delta_{11}}\right) - \mu_{MDC} MDC \tag{1.16}$$

Note the constant φ represents a scaling factor between compartmental measuring units of the lung and the DLN and is strictly linked to the measure units used in the model according to experimental data available (we addressed this point in the *Measure units* section).

2.2.5. Immature DC in the lung (IDC)

Immature or resident DCs (Eq. (1.17)) are normally present in the lung (approximately 10% of resident macrophage population, i.e. 5×10^4) with a natural turnover (as resident macrophages) (Holt, 2000; Holt and Stumbles, 2000a, b). They are governed by a source (s_{IDC}) of new cells migrating into the site and a natural death of cells (at rate μ_{IDC}). With no infection, the dendritic cell population should remain at equilibrium, IDC $= s_{IDC}/\mu_{IDC}$. During infection, IDCs undergo two different dynamics: further recruitment (induced by a chemokine gradient) and maturation/migration to the DLN. Recruitment (at the maximal rate δ_8) and maturation/migration (at the maximal rate δ_{10}) are triggered by bacterial invasion (expressed by the concentration of extracellular bacteria B_E).

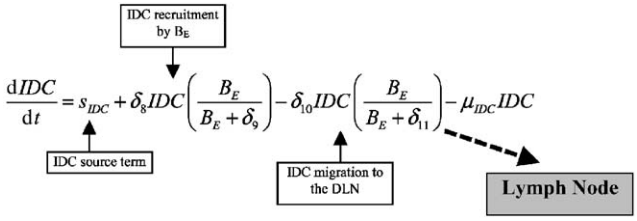

$$\frac{dIDC}{dt} = s_{IDC} + \delta_8 IDC\left(\frac{B_E}{B_E + \delta_9}\right) - \delta_{10} IDC\left(\frac{B_E}{B_E + \delta_{11}}\right) - \mu_{IDC} IDC \tag{1.17}$$

2.3. Numerical simulations

2.3.1. Parameter estimation

Once the model is developed and before simulations are performed, rates for each of the dynamics must be estimated. Rates of interactions and kinetics are estimated from published experimental data and are presented in the appendix. Human-derived experimental data and non-human primate (NHP) data are used in estimations when possible. Other animal data (mouse, rabbit) are used to derive magnitude estimates when no human or primate data are available. In the absence of data, mathematical estimation is used (see appendix for a discussion of parameter estimation).

Regardless, all parameters are evaluated using uncertainty and sensitivity analyses performed with C code

based on Latin hypercube sampling (LHS) and partial rank correlation (PRC), respectively (Blower and Dowlatabadi, 1994; Greenland, 2001; Helton and Davis, 2002; Sanchez and Bowler, 1997).

2.3.2. Uncertainty and sensitivity analyses

There are variances in many of the parameter values due to extensive variability in data. Such variances require an evaluation of the uncertainty in the system. We employ the LHS method to assess effects of uncertainties in our parameter estimation on model outcomes. LHS allows for simultaneous random, evenly distributed sampling of each parameter within a defined range. A matrix consisting of m columns corresponding to the number of varied parameters and n rows for the number of simulations, is generated; n solutions are created that show uncertainty in model outcomes due to parameter variations. By combining the uncertainty analyses with PRC, we are able to reasonably assess the sensitivity of our outcome variables to parameter variation. This allows us to identify and quantify critical parameters (i.e. interactions) that dramatically affect the outcome when varied.

2.3.3. Computer simulations

Once we derive the model and estimate parameters, we solve the system of ordinary differential equations (ODEs) to obtain temporal dynamics for each variable. To this end, we use MatLab's[4] ode15 s solver for stiff systems (Klopfens.Rw, 1971) for solving the system of ODEs. We compare results with those generated from a numerical algorithm using C code of a stiff adaptive solver based on the Rosenbrock and Storey method (Rosenbrock and Storey, 1970) for consistency (generated in our group).

We run virtual model simulations using different sets of parameter values. The system is able to reproduce expected infection outcomes, namely: latency, primary TB ("slow" and fast progression), clearance and reactivation. We also obtained a very rapid clearance scenario (data not shown): a few inoculated bacteria are readily cleared by innate immunity in a few days. The complete list of parameters is given in the appendix where we specify the values that we use to achieve latency.

Each block of figures to follow represents the immune response at the site of infection of lung (A) and in the draining lymph node environment (B) for different infection outcomes. In general, Panels A comprise four subplots describing, respectively, macrophage populations, cytokine concentrations, Th1 and Th2 cells and bacterial subpopulations. Panels B illustrate DC dynamics, naïve T cells, IL-12 in the DLN and Th precursor trafficking. Although Th_P^{LUNG} and IDC belong to the lung compartment, they have been included in Panels B in order to compare trafficking and migration patterns of DCs and Th precursors between the lung and the DLN.

Finally, different infection outcomes are obtained by varying parameter values. There likely exists a function for the classical R_0 determining an expression for transition between infection outcomes. Since the model is too complex to obtain such an expression, we rely on our uncertainty and sensitivity analysis to identify relevant bifurcation parameters. Because we wish to maintain the biological integrity of the system, we cannot vary parameter outside their relevant range of values. Thus, obtaining these three distinct outcomes does not depend on a unique set of parameters but rather on combined ranges.

After the outcomes are presented, we discuss in detail the sets of parameters that are responsible for leading to the different disease trajectories observed. It is the host–pathogen processes governed by these parameters that are likely targets for further basic science study.

2.3.4. Measure units: scaling lung and lymph node compartments

Our system is developed to model human TB both at the site of infection and in the draining lymph node. In the lung model (Wigginton and Kirschner, 2001), the reference space for the site of infection is the bronchoalveolar lavage (BAL) fluid.

BAL measures have some drawbacks. Firstly, they overestimate macrophage population size and activity (for example, cytokines production) in the lower respiratory tract, in particular, underestimating DC and lymphocyte populations. Certainly BAL samples cannot be performed in the DLN and thus are not very informative regarding lymph node environment. Finally, tuberculosis is a disease involving primarily the lung parenchyma, rather than the airways. Cells and cytokines present in BAL fluid likely do not accurately reflect the composition of the lung. However, the limitations of the human system do not permit sampling of lung tissue, and BAL is the only available alternative.

In order to scale lung and lymph node compartment cell trafficking, we use volumetric measure units, namely cells per cm^3 of tissue (both in the lung and in the lymph node) (Choi et al., 2001).

We calibrate initial conditions of our virtual model to match estimates of cell distributions in the two compartments (Table 2). The bold values in Table 2 represent initial conditions for macrophages and DCs (column 2). Since we want to mimic trafficking into and out of the lymph node compartment, we assume very low lymphocyte levels from the start of our study (10^3 naïve T cells). The initial bacterial load is 25 bacteria.

Each equation of the virtual model thus represents the incremental variation of a certain quantity over time

[4] Version 6.5, R13, Copyright 1984–2002, The MathWorks, Inc.

Table 2
Cell distribution (in percentages) by compartment (lung and Hilar lymph node) with no infection. Data are deduced from the literature (references). Lung and Lymph Node measures are normalized over 10^6 and 10^4 cells, respectively

Cell types	Lung[a]	Hilar lymph node[b]
Macrophages[c]	0.4–0.5 (4.0–**5.0** × 10^5)	0.05–0.1
DCs	0.05–0.1 (**5.0**–10.0 × 10^4)	0.05–0.1
Lymphocytes	0.05–0.1	0.8–0.9 (8.0–9.0 × 10^3)
Other (NKs, PMNs, etc.)	0.35–0.45	—

[a] Holt and Schon-Hegrad (1987), Holt (2000), Holt and Stumbles (2000a, b), Stone et al. (1992), Mercer et al. (1994).
[b] Young and Hay (1999), Young (1999).
[c] Law et al. (1996), Condos et al. (1998), Antony et al. (1993), Schwander et al. (1998).

(day): pg/ml ($\times 10^6$ cells) for cytokine concentrations and cell/cm^3 of tissue for the cellular variables (we convert back to cells/ml for ease of reporting).

2.3.5. Markers of *M. tuberculosis* disease progressions in humans

When active TB develops, disease localization, severity, and outcome are highly variable and little data exist on timing of infection. A positive purified protein derivative (PPD+) test status indicates infection. Progression from negative to positive PPD test means progression from exposure to infection. Because of the wide time range in which disease can progress to an active state, primary TB ranges from 1 to 5 years (Comstock et al., 1974). This represents the time frame within which patients who have been exposed to *M. tuberculosis* progress to a state where disease is manifested. Treated, such patients usually recover. Untreated, the outcome could be death, or a protracted chronic infection. Spontaneous recovery can occur, but is a lengthy process. Individuals exposed to bacilli but who do not progress to active disease (i.e. in the 1–5 years after infection) are generally believed to contain dormant bacilli; this state is often referred to as latent tuberculosis (Bloom, 1994).

What remains to be defined is a marker of disease progression. No good markers of TB progression in humans presently exist. Sputum samples are positive for mycobacteria in people with active TB and when an infected person is treated with anti-tuberculosis therapy, it is standard to look at conversion to sputum culture negativity. So, by inference, bacterial load is likely a good marker of TB progression. For example, a treated person whose positive sputum converts to negative and later turns positive either has relapse or exogenous reinfection. In the mouse, bacterial burden (in the whole lung) greater than 10^8 translates to death (Bloom, 1994). Whether an equivalent threshold exists for humans is unclear. Bacterial load has been shown to be useful in NHPs, where colony-forming units (CFUs) in tissues correlate with disease status (Langermans et al., 2001). CFU is a good readout since if it increases, it indicates a failure in some aspect of the immune response.

In our simulations, we consider total bacterial load as the most informative marker of disease progression. Due to the crucial role of macrophages in *M. tuberculosis* infection, the absolute and relative levels of resident, infected and activated macrophages are also useful.

3. Results

3.1. Baseline simulation: no infection

If we specify basal initial conditions for lung tissues (see Table 2, normal levels of resting macrophages and immature DCs, with all the initial conditions of the rest of the variables set to zero), the model mimics the immune system in its dormant state, with levels of macrophages and IDCs consistent with baseline levels detected in normal healthy lung tissues (Holt and Schon-Hegrad, 1987; Holt, 2000; Holt and Stumbles, 2000a, b) (data not shown). If a few bacteria are inoculated, the model will progress either to clearance, latency or primary TB (fast or slow progression), depending on different sets of values for parameters in the model. The complete list of baseline parameters and their ranges is given in the appendix, while different simulation results and their parameter sets are discussed below.

3.2. Primary TB

Figs. 2A and B present the results of primary TB in our virtual model simulations. The velocity of infection progression depends on the initial bacterial load: in this simulation, the inoculum was 25 mycobacteria, but if the initial burden is increased, progression to either latency or primary TB is faster (data not shown). This suggests that the wide time range (1–5 years) within which individuals progress to active disease might be dependent on the initial dose as well as other factors (see below).

After a small number of bacteria enter the host, the resting macrophage population undergoes slow steady infection that is supplemented by newly recruited monocytes that differentiate into resting macrophages soon after they reach the site of infection. Because of rapid turnover of resident lung macrophages, the macrophage population is relatively stable during the first weeks, although the population of infected and activated macrophages increases. Th precursor dynamics also are initiated in the DLN, inducing a

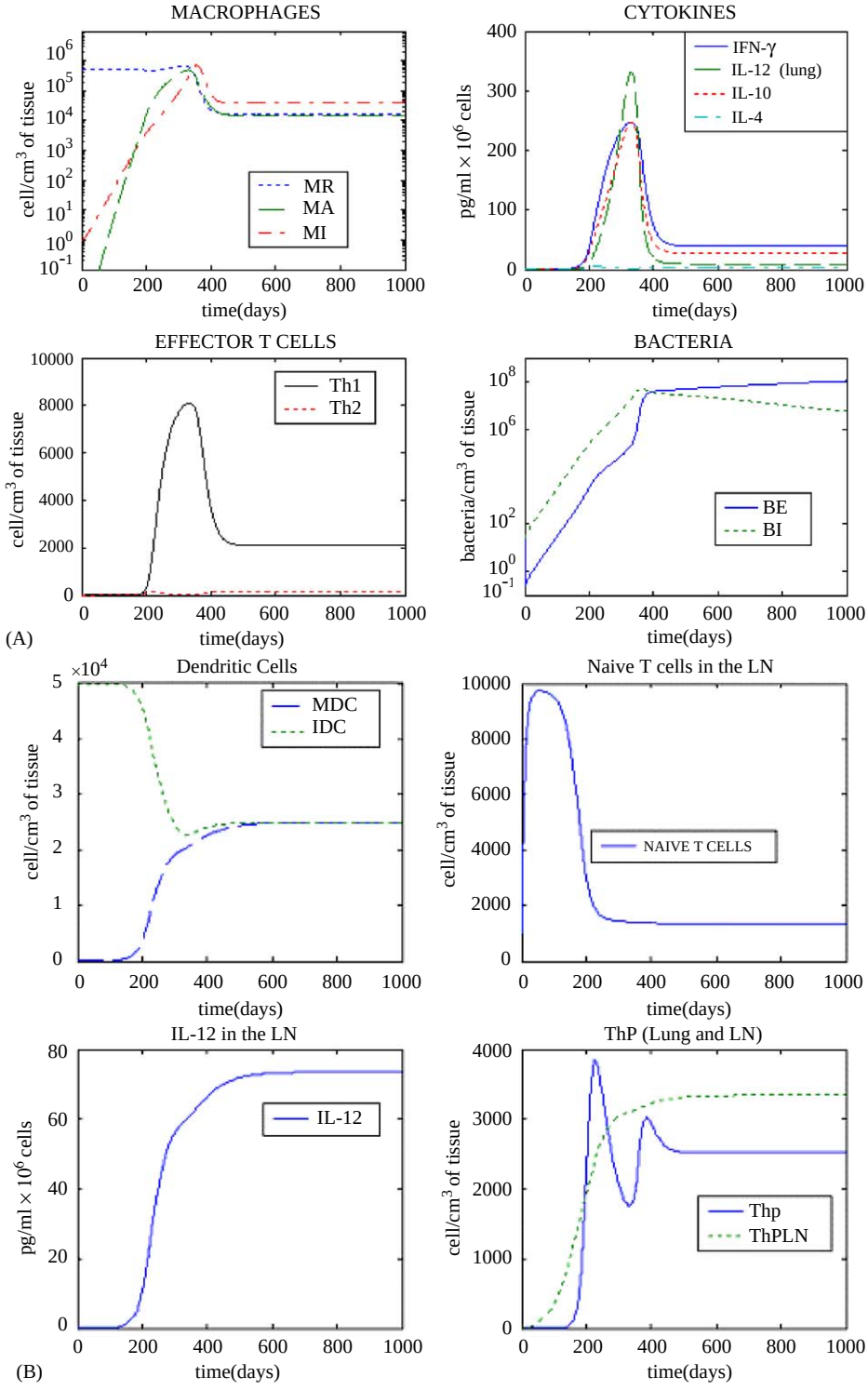

Fig. 2. (A) Lung population dynamics (macrophages, cytokines, Th1/Th2 and bacteria) during primary TB (we use the parameter values given in the Appendix, except for $k_{14} = 1.6$, $k_6 = 1e{-}5$, $k_7 = 0.02$, $\alpha_{20} = 0.0005$, $\delta_{12} = 4e{-}5$, $\delta_{11} = 100$) Macrophage and bacteria populations are in log scale. (B) Draining lymph node dynamics (IDC and MDC, Naïve Ts, IL-12, both ThP in the lung and the DLN) during primary TB (we use the parameter values given in the Appendix, except for $k_{14} = 1.6$, $k_6 = 1e{-}5$, $k_7 = 0.7$, $\alpha_{20} = 0.0005$, $\delta_{12} = 4e{-}5$, $\delta_{11} = 100$).

migration pattern of helper T cells to the site of infection before approximately 2–3 weeks.

After 200 days, high levels of infected and activated macrophages trigger recruitment of new resting macrophages, resulting in a higher threshold in the total number of intracellular bacteria. After approximately 1 year, a switch in the immune response occurs (Fig. 2A): intracellular bacteria proliferate beyond the maximal

capacity N (MOI) of chronically infected macrophages, inducing bursting and subsequent release of large amounts of bacteria. As a result, total bacterial load grows without control (greater than 10^8 bacteria/cm^3 in less than 3 years). This high total bacterial load likely leads to necrosis, cavity formation and dissemination (eventually with death of the host).

Cytokine levels reflect macrophage dynamics: IL-12, IFN-γ and IL-10 peak after 1 year (with IL-4 always very low, almost undetectable levels), and then rapidly decrease. Effector T cell and macrophage populations induce cytokine dynamics, leading to an extremely active Th1-response between 200 and 500 days (Fig. 2A). Th1 cells peak at 8×10^3 cells/cm^3 after 1 year, and then decrease rapidly to a steady state (approximately 2×10^3 cells/cm^3), unable to contain infection resulting in uncontrolled disease progression. Th2 responses remain very low and relatively stable.

Th precursor cells in the draining lymph node increase to steady state (in 1 year) at around 3.2×10^3 cells/cm^3. They migrate into the blood, increasing the Th precursor population in the lung compartment as soon as activated macrophages release consistent amounts of chemokines. A large influx of Th_P at the site of infection (Th_P^{LUNG}) occurs at 200 days, stabilizing at 2.5×10^3 cells/cm^3. After 1 year Th precursor cells in the DLN are greater than in the lung (around 40% higher), likely indicating defective trafficking capabilities into the blood. This may be due to very low chemokine concentrations at the site of infection as a result of the decrease in healthy macrophages.

DC trafficking clearly shows a balance between IDCs migrating out of the site of infection and MDCs entering into the DLN (Fig. 2B). As a result of antigen uptake, IDCs mature and migrate to the DLN: IDCs at the site of infection decrease and reach a steady state, at around 2.5×10^4 cells/cm^3 (after approximately 1.5 years after infection), 50% lower than the initial condition (assumed baseline). Conversely, MDC levels in the DLN increase and overlap IDCs. IL-12 concentrations in the DLN follow MDC population dynamics, increasing in the first year and then reaching a steady state (around 70 pg/ml). Naïve T cell recruitment is very fast in the first month (with a peak at 10^4 cells/ml), decreasing and stabilizing around 1.5×10^3 cells/cm^3 at day 400.

3.3. Latency

The initial stages of latency are similar to primary TB up to day 250, but now a sustained macrophage activation (10-fold higher than primary TB) results in 100-fold lower levels of intracellular bacteria, at about 4×10^5 cells/cm^3. The number of infected macrophages is small and total bacterial load is basically represented by intracellular bacteria (extracellular bacterial load is almost zero after 1000 days). Extracellular bacteria are readily internalized by both macrophages and IDCs and are also killed by activated macrophages, thus containing infection. The system is completely under control and latency is achieved at approximately 200 days. Overall, there is a 60% increase in healthy resting macrophages in the lung.

Cytokine levels are predominantly of type 1 and are sustained after latency has been achieved. IL-10 adequately regulates IFN-γ and IL-12 activity, down-regulating macrophage activation. These cytokines reach a stable level, with IFN-γ (1.4×10^2 pg/ml) 2-fold higher than IL-12. IL-4 levels are 20–30-fold lower than IL-12.

In the first year, IFN-γ levels in primary TB are 2.5-fold higher than during latency. Once latency is achieved (after a year), IFN-γ levels are 3-fold higher than in primary TB, suggesting an important role for activated macrophages in killing bacteria and containing infection. A protective Th1 response is mounted after 200 days, with cells peaking at 3.7×10^3 cells/cm^3 after 1 year and then decreasing to very low levels once latency has been established (Fig. 3A). Although very low, these levels are crucial to latency. During latency, lymphocyte populations present in the lung are mainly Th precursors, with very low levels of both Th1 and Th2 cells. These very low levels may also indicate that helper T cells are present at the site of infection but they are not continually receiving sufficient stimuli to become fully differentiated and exert their effector function. During the first 200 days, the dynamics of the Th precursor cells are similar to primary TB. After 200 days, Th precursor cells in the draining lymph node start to decrease (from the peak of 3×10^3 to 10–15-fold lower than primary TB, down to $2–3\times10^2$ cells/cm^3), while Th precursors in the lung continue increasing (up to 5×10^3 cells/cm^3) and remain higher than those in the DLN, stabilizing much later than other cells in the system (Fig. 3B). This suggests that during peak infection, comparing latency to primary TB, a faster migration of Th precursor cells from the DLNs to the lung (2-fold higher in latency, due to the larger amounts of chemokines released by activated macrophages at the site of infection) may explain the host ability to contain bacteria in the latency outcome.

DC trafficking and presentation are enhanced and sustained, although much less than primary TB. DC levels return to baseline after latency is achieved (Fig. 3B). IDCs at the site of infection, after an initial large migration, return to their initial size (5×10^4 cells/cm^3), suggesting how the role of DC is necessary for both establishing latency (via MDC presentation in the DLN) and maintaining latency (via IDCs as sentinels for further extracellular bacteria invasion).

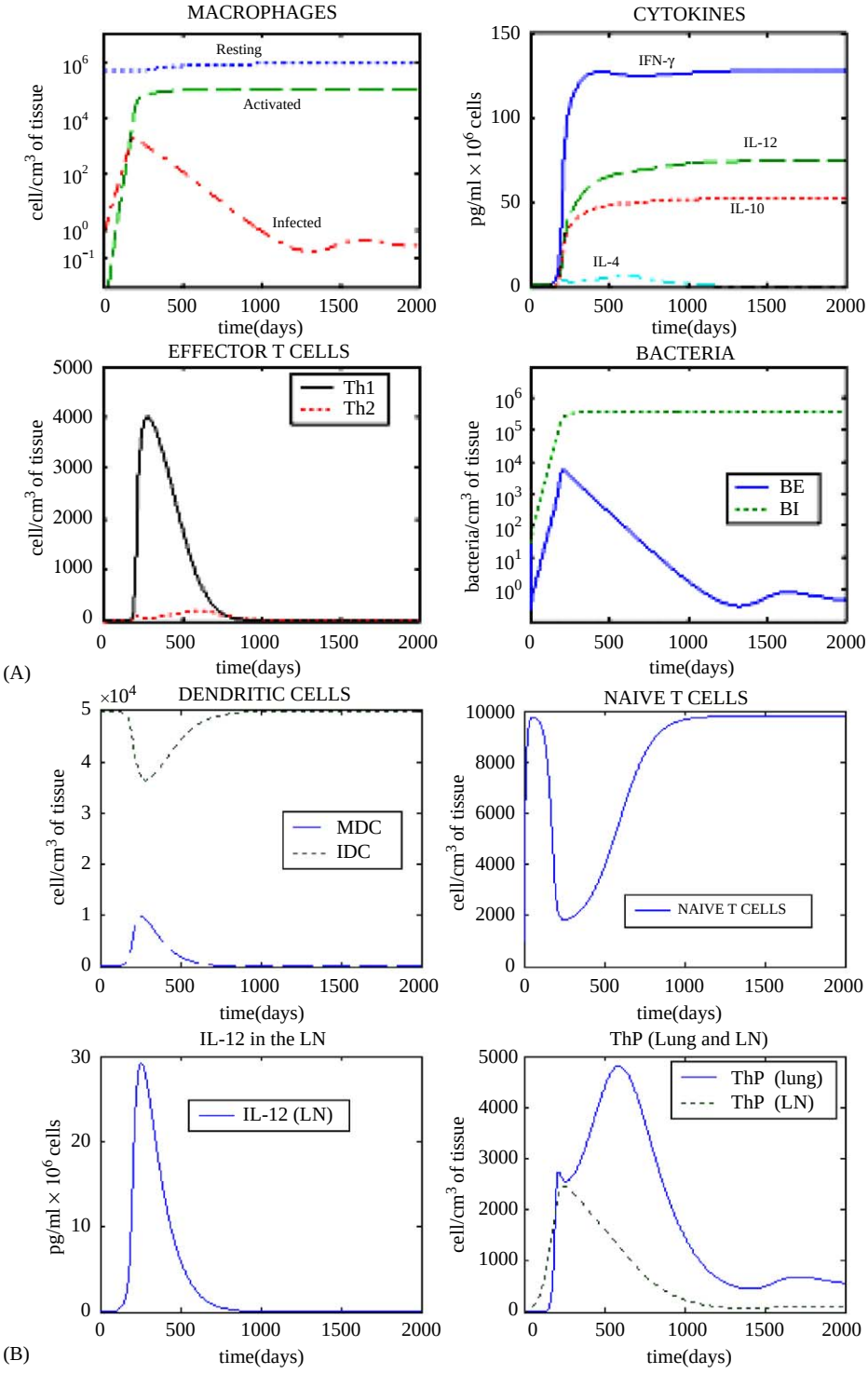

Fig. 3. (A) Lung population dynamics (macrophages, cytokines, Th1/Th2 and bacteria) during latency (1000 days). Macrophage and bacteria populations are in log scale. (B) Draining lymph node dynamics (IDC and MDC, Naïve Ts, IL-12, both ThP in the lung and the DLN) during latency (2000 days).

3.4. Primary TB (rapid progression)

We also obtain two other possible scenarios with our virtual model simulations (data not shown): a rapid progression to primary TB and clearance. Rapid progression to primary TB might be the result of an immunocompromized host or of a particular virulent strain of mycobacteria. Failure of innate immunity is likely to induce this, resembling the primary TB outcome (Fig. 2) but disease progression is faster, with

extracellular bacteria increasing to uncontrollable levels (10^8 bacteria/cm^3) after 200 days and DLN dynamics are not fast enough to contain the initial wave of infection.

3.5. Clearance

There are hypothetically two types of clearance: a PPD negative scenario where a person who is exposed and infected clears the bacteria before any adaptive immunity is elicited (innate immunity action, very early, no Th1 response), and a PPD positive scenario where the infection is cleared by adaptive immunity and memory is retained. Although clearance in *M. tuberculosis* infection is likely a result of a strong innate response rather than an adaptive immunity phenomenon, we obtain both types of clearance. In particular we obtain clearance of mycobacteria after less than 1 year with all cells returning to baseline levels (Fig. 4). Innate immunity (mainly resting macrophages and IDCs) plays a key role: comparing to latency (Figs. 3), both a higher (10-fold) recruitment rate of macrophages and higher IDCs bacterial uptake rate, coupled with a more effective (100-fold stronger) phagocytosis and killing by macrophages, results in clearance. A very low level of immune response is able to clear both extracellular and intracellular bacteria (PPD+). This scenario may induce reactivation if few bacteria are present at the site of infection (data not shown).

3.6. Reactivation

We also define a possible reactivation scenario. Although it is likely a perturbation of latency that induces reactivation (see Wigginton and Kirschner, 2001), we obtained a very slow chronic infection with controlled bacterial growth, resembling reactivation. A low but steady loss of immune efficiency (e.g. less macrophage and T cell killing) coupled with a slower macrophage infection rate and extracellular bacterial growth rate, lead to high levels of bacteria (Fig. 4C) within a time frame of 30 years (10,000 days). We note lower levels of IL-12 and IFN-γ in the lung, comparing to latency, while IL-10 is the same.

3.7. Differences in the infection outcomes

In order to understand how different sets of parameter values lead to different infection outcomes,

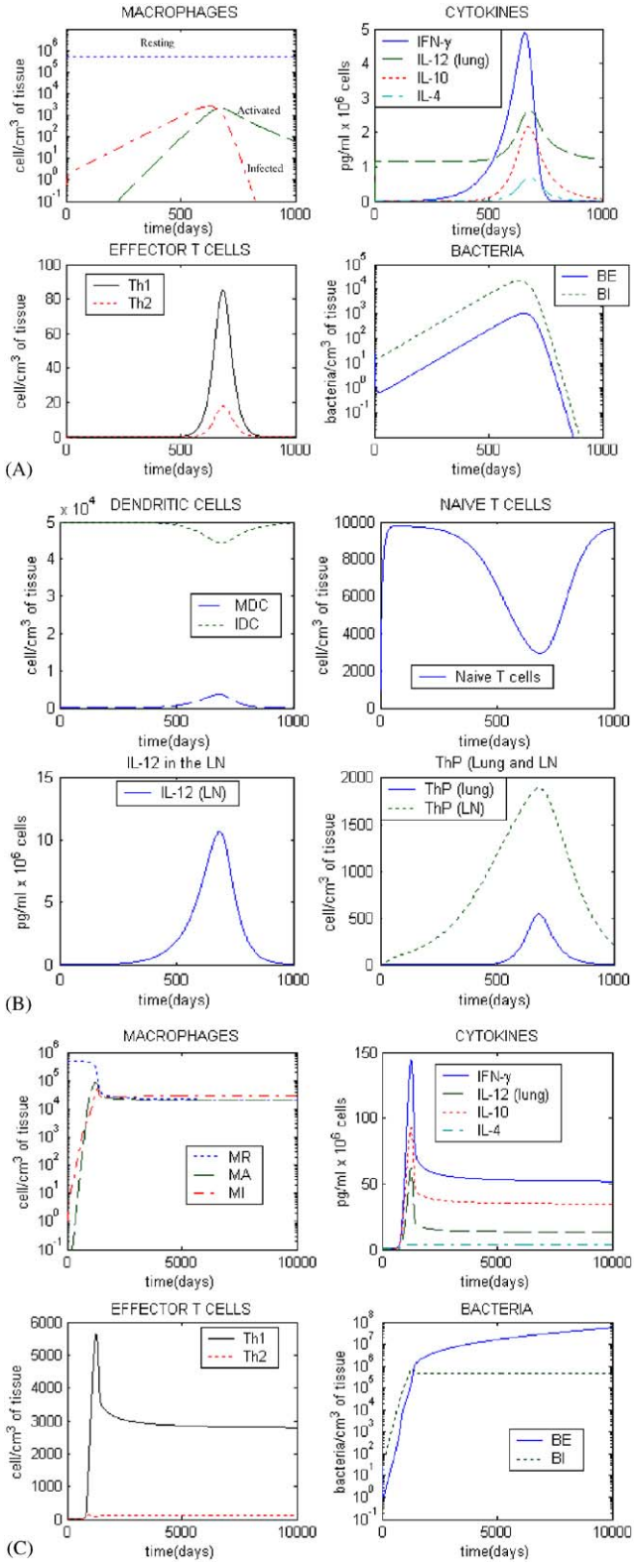

Fig. 4. (A) Lung population dynamics (macrophages, cytokines, Th1/Th2 and bacteria) during PPD+ clearance (we use the parameter values given in the appendix, except for $\alpha_2 = 0.14$, $k_6 = 1e{-}1$, $\delta_1 = 0.035$, $\delta_{10} = 0.2$). Macrophage and bacteria populations are in log scale. (B) Draining lymph node (IDC and MDC, Naïve Ts, IL-12, both ThP in the lung and the DLN) during PPD+ clearance (we use the parameter values given in the appendix, except for $\alpha_2 = 0.14$, $k_6 = 1e{-}1$, $\delta_1 = 0.035$, $\delta_{10} = 0.2$). (C) Lung population dynamics (macrophages, cytokines, Th1/Th2 and bacteria) during reactivation (10,000 days) (we use the parameter values given in the appendix, except for $k_6 = 1e{-}3$, $k_7 = 0.1$, $\alpha_{20} = 0.016$, $\delta_{12} = 1e{-}6$, $\delta_{11} = 100$, $\delta_1 = 0.035$, $\delta_{10} = 0.2$). Macrophage and bacteria populations are in log scale.

we classify model parameters into four groups, namely: infectivity, presentation/activation/differentiation, trafficking and uptake/killing parameters (see Table 3).

The parameter space has been explored to assess which parameter (single effect) or which combination of parameters variations (multiple effect) might distinguish between different disease trajectories (clearance, latency or primary TB). The baseline trajectory is the one leading to latency (column 2, Table 3).

Two parameters are crucial in determining infection outcome: the infection rate of resident macrophages by extracellular bacteria (k_2) and T-cell killing of infected macrophages by apoptosis and cytotoxic action (k_{14}). Although the model does not explicitly include CTL cells, k_{14} represents a combination of both Th1 apoptosis and CTL-induced killing.

Both an increase in macrophage infection rate (k_2) and a decrease in T-cell effector immunity (k_{14}) result in primary TB. On the other hand, decreasing the infection rate of resident macrophages (k_2) results in clearance and increasing T-cell killing of infected macrophages (k_{14}).

Due to the large number of equations and parameters in the model we use our uncertainty and sensitivity analyses to assess which parameters contribute to outcome variability (defined here as total bacterial load). In particular, we investigate the nature of transitions between different infection outcomes: latency to disease and latency to clearance. To this end, we present a plot of different bacterial load dynamics based on variable parameter inputs. Fig. 5A illustrates how the variation in macrophage infection rate (k_2) affects the gradual transition from latency to active TB (represented in the figure by total bacterial load).

A switch from latency to primary TB can also be induced by either increasing the extracellular bacterial growth rate (α_{20}) or by decreasing the activation rate of resting macrophages induced by the product of total number of bacteria (B_T) and by IFN-γ (k_3) (see Table 3).

These results are in line with the results from our lung model sensitivity analysis (Wigginton and Kirschner, 2001), where five parameters were found to be key in determining different infection outcomes.

Table 3
Parameter classification (parameter definitions are given in column 1) and sensitivity analysis performed over specified parameter ranges (column 2). Increasing or decreasing certain parameters (column 3), leads the system from latency (parameter values for latency are given in parenthesis in column 2) to either clearance or disease (column 4)

Parameters	Biological Range	Action	Event
Infectivity parameters			
k_2 (M_R infection due to B_E)	0–1 (0.4)	Increase	From latency to disease
k_2 (M_R infection due to B_E)	0–1 (0.4)	Decrease	From latency to clearance
α_{20} (B_E growth rate)	0–0.5 (0.005)	Increase	From latency to disease
Presentation/activation/differentiation parameters			
k_3 (M_R activation, induced by B_T and IFN-γ)	0.01–0.95 (0.4)	Decrease	From latency to disease
k_4 (M_A deactivation, induced by IL-10)	0–1 (0.36)	Increase	From latency to disease
IFN-γ production: sg (extra source)	0–1000 (700)	Decrease	From latency to disease
δ_1 (IL-12 production by MDC, in the DLN)	0–1.0e−1 (0.0035)	Decrease	From latency to disease
μ_{MDC} (MDC death and exhaustion rate)	0–1 (0.02)	Increase	From latency to disease
k_6 (Th1 differentiation)	0–1.0 (0.1)	Decrease	From latency to disease
k_7 (Th2 differentiation)	0–3.0 (0.05)	Increase	From latency to disease
δ_4 (MDC-T cell interactions: T cell activation)	0–1e−1 (0.0001)	Decrease	From latency to disease
Trafficking parameters			
ξ (% of precursor helper T cells migrating out of the DLN into the blood	0–1 (0.9)	Decrease	From latency to disease
s_{IDC} (IDC normal turnover in the lung)	0–1000 (500)	Decrease	From latency to disease
δ_{10} (IDC activation/migration/maturation from the Lung to the DLN)	0–1 (0.02)	Decrease	From latency to disease (high levels of B_I and B_E, 10^7)
δ_{10} (IDC activation/migration/maturation from the Lung to the DLN)	0–1 (0.2)	Increase	From latency to B_I 10-folds lower
Uptake/killing parameters			
δ_{12} (IDC uptake of B_E)	0–1e−5 (1.00E−07)	Increase	From latency to clearance
k_{14} (T cell killing of M_I: apoptosis, CTL)	1.6e−3–2.6 (0.5)	Increase	From latency to clearance
k_{14} (T cell killing of M_I: apoptosis, CTL)	1.6e−3–2.6 (0.5)	Decrease	From latency to disease
k_{15} (B_E killing by M_A)	0–1e−5 (1.25E−07)	Increase	Latency, with lower levels of BI (10–20-folds lower)
k_{18} (B_E killing by M_R)	0–1e−5 (1.25E−08)	Increase	From latency to clearance

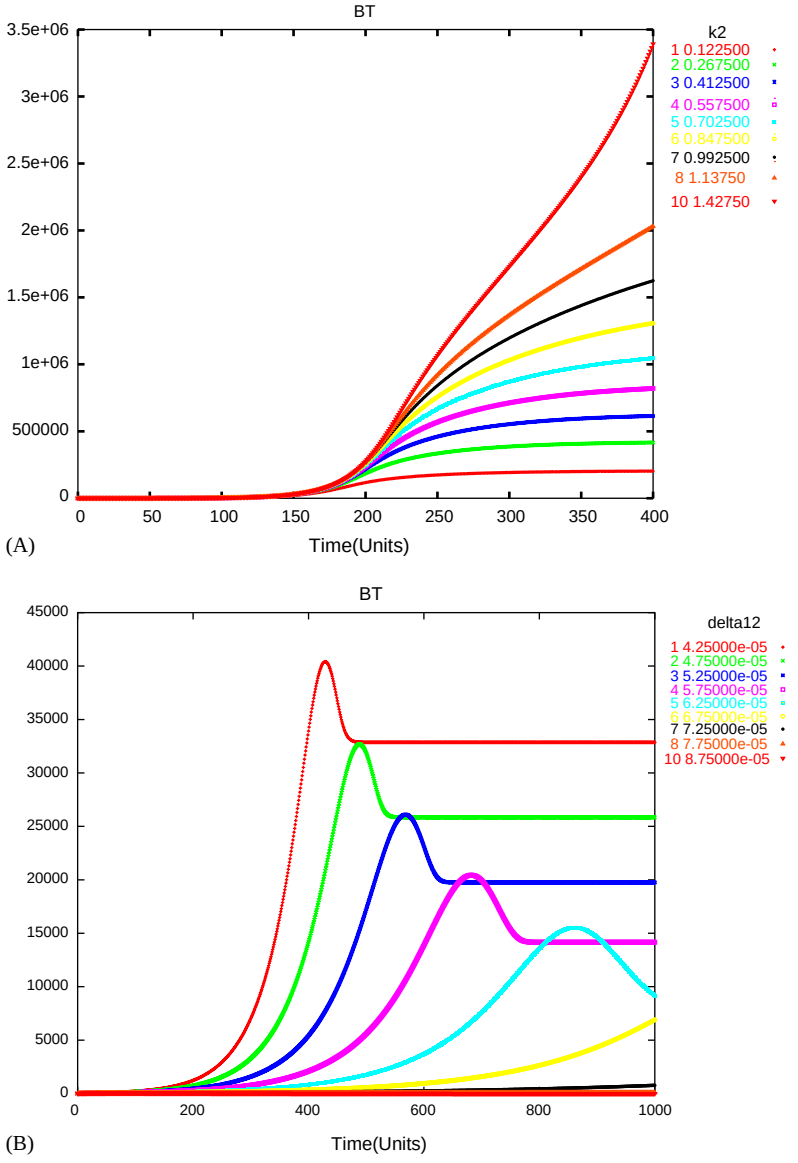

Fig. 5. (A) Plots of total bacterial load (BT) varying the rate of infection of resting macrophages due to extracellular bacteria (parameter k_2) over a specified range [0–1.5]. Plot shows the gradual nature of transition from latency to active TB. (B) Plots of total bacterial load (BT) varying the rate of extracellular bacteria uptake by immature DCs (parameter δ_{12}) over a specified range [4e−5–1e−4]. It shows the gradual nature of transition from latency to clearance.

Two other parameters were previously relevant in the lung model but are not determinant in the new model outcomes: IL-4 production by Th precursor cells (α_{11}) and the death rate of resting macrophages (μ_R). The reason why the death rate of resting macrophages is not determinant in the new model might be that IDCs balance macrophage loss. The key-role of IL-4 in enhancing Th2 differentiation and down regulating Th1 differentiation is better represented in our new model (see the end of this section) and may be why this specific parameter is no longer determinative.

In the new model, increasing values for extracellular bacteria growth and the rate of macrophage activation (α_{20} and k_2, respectively) could represent a virulent strain of mycobacteria (van Crevel et al., 2002) resulting in primary TB (or fast progression, depending on the situation of the host and on the initial bacterial load). This effect is strengthened when coupled with low values of bacterial killing by activated and infected macrophages (k_{15} and k_{18}, respectively), resulting in a successful *M. tuberculosis* colonization of the host.

Plots in Fig. 5B shows the transition from latency to clearance (summary in Table 3) when uptake rate of bacteria by IDCs (δ_{12}) is changed. Effective innate immunity, represented by increasing levels of both killing of bacteria by resident macrophages (k_{18}) and uptake rate of bacteria by IDCs (δ_{12}), leads to clearance.

Clearance is also achieved by decreasing the deactivation rate of activated macrophages (k_4) which is driven by IL-10. Decreasing the extra source of IFN-γ (s_g), leads to primary TB, emphasizing the role of CD8 + T cells and possibly NK cells in a protective Th1 response to *M. tuberculosis*. This is explored more fully in other work.[5]

The necessary (although not sufficient) Th1 protective immunity is confirmed by the importance of parameters governing Th1 and Th2 differentiation (k_6 and k_7, respectively) which show how a switch from latency to primary TB results from either a decrease in the Th1 differentiation rate (k_6) or increasing the Th2 differentiation rate (k_7), suggesting how a Th1/Th2 balance is desirable and how a Th2 response is not protective in *Mtb* infection.

A more detailed analysis of trafficking and antigen presentation dynamics (focused on DCs) is discussed in another paper[6] from our group.

3.8. Treatment

Treatment of TB is administered both prophylatically to latently infected individuals to reduce risk of reactivation and therapeutically to those with active disease (to induce latency). Because bacteria may potentially survive for decades intracellularly, antibiotics are typically given for periods as long as 2 years (Iseman, 2002). Through the use of multi-drug treatment regimen, a 6–9 months course may be all that is required; however, due to non-compliance or abandonment emergence of multi-drug resistant (MDR) TB poses a world threat that has not gone unnoticed by the WHO (International Union against Tuberculosis and Lung Disease. World Conference; Iseman, 1999a, b).

The future of TB treatment may require improved antibiotic efficacy which may be accomplished by strengthening either the *early bactericidal activity* (EBA) or the *late sterilizing effect* that kills bacteria in a dormant state of metabolism (latency).

Following (Kirschner, 1999), we incorporate treatment by affecting key parameters of the model. Because we have performed a complete uncertainty and sensitivity analysis on all parameters in the model (Table 3) we can predict the effects treatment will have on the system. For example, increased EBA can be achieved by inducing a stronger innate response, i.e. increasing the number of immature dendritic cells (higher s_{IDC}) as well as the killing capability of IDC and resident macrophages at the site of infection (higher values of δ_{12} and k_{18}, respectively). *Late sterilising effects* could be similarly reproduced by enhancing migration and presentation in lymph node: again DCs could be potential vectors for therapy since they are better equipped than macrophages in containing Mtb proliferation and migrate to the lymph node after contact with bacteria. This eventually results in a more efficient T-cell mediated immunity, namely Th1 and CTL activity, that targets residual intracellular bacteria and prevent reactivation.

[5] Dhruv Sud and Denise Kirschner (submitted Jan 2004), The role of TNF-α and CD8+ T cells in controlling *Mycobacterium tuberculosis* infection.

[6] Simeone Marino, Joanne L. Flynn, Denise E. Kirschner (submitted October 2003), Dendritic Cell Trafficking And Antigen Presentation In The Human Immune Response To *Mycobacterium tuberculosis*.

4. Discussion

In this paper we have presented an updated version of a previously published (Wigginton and Kirschner, 2001) virtual model of the immune response to *M. tuberculosis*. Our new model addresses the relevance of two compartments: the site of infection (lung) and the secondary lymphoid tissue (lymph node) and further explores the complex regulatory immune network by including dendritic cells and their trafficking.

After entry into the human lung, *M. tuberculosis* has a series of encounters with different host defense mechanisms. The progression and the final outcome of infection depend on the balance between outgrowth and killing of *M. tuberculosis*.

Our model suggests how clearance depends on the intrinsic microbicidal capacity of host phagocytes and on virulence factors of the ingested mycobacteria. Increasing innate immunity mechanisms of the model, i.e. killing of bacteria by resident macrophages and the internalization of bacteria by IDCs, induces fast clearance (data not shown) with no memory of adaptive immunity (PPD negative). On the other hand, by increasing virulence factors of the ingested mycobacteria, i.e. the extracellular growth rate and the infection rate of resident macrophages by extracellular bacteria, we obtain primary TB, the velocity of which depends on the initial bacterial load (data not shown), as well as on a series of other factors, including T cell killing of infected macrophages by apoptosis and cytotoxic action, activation of resting macrophages induced by the total number of bacteria and by IFN-γ action, as well as macrophage deactivation induced by IL-10. Our model also distinguishes the mechanisms for fast primary TB progression. This scenario could occur under conditions of failing immune surveillance (like AIDS or immunocompromised) or when the initial bacterial burden is considerably large or particularly virulent. Recent epidemiological data (Crowle and Elkins, 1990; Stead et al., 1990), genetic studies (Bellamy et al., 1998, 1999; Fenhalls et al., 2002; Wilkinson et al., 1999, 2000) and both clinical and experimental results support a role for innate immunity as well as the relevance of T-cell-independent, intrinsic bactericidal activity of

macrophages in human tuberculosis (van Crevel et al., 2002).

We also define two possible reactivation scenarios. We obtained a very slow chronic infection where a low but steady loss of immune response efficiency is coupled with a slower macrophage infection rate and extracellular bacterial growth, leading to very high bacteria levels within 30 years. Another possible reactivation outcome may be caused by down-regulating key parameters (in particular DC turnover, presentation and half-life), thus reactivating mycobacteria infection and leading to death in a shorter time as compared to the first reactivation scenario.[7]

We also observed dynamics of early stages of infection by varying the temporal frame of the simulation to determine whether significant differences exist between different infection outcomes (data not shown). The model does not show any particular difference during early stages of infection between latency and active TB (as long as a reasonable inoculum is considered, data not shown). It is likely that the study of spatial patterns of granuloma is needed to understand these early infection dynamics. In other work we have investigated the spatial organization of the immune response to TB in the lung using three different mathematical frameworks: a partial differential equation model (Gammack et al., 2003), a metapopulation model[8] and an agent base model.[9]

Considering Th1/Th2 differentiation, controversial results can be found in the literature regarding T-cell population during *M. tuberculosis* infection in the lung. An increase in Th2-type cytokines in tuberculosis patients has been reported (Bhattacharyya et al., 1999; Dlugovitzky et al., 1999; Seah and Rook, 2001; Surcel et al., 1994; van Crevel et al., 2000). However, this is not a consistent finding (Barnes et al., 1993; Hernandez-Pando and Rook, 1994; Jung et al., 2002; Lai et al., 1997; Lin et al., 2000), and the relevance of the Th1/Th2 concept in *M. tuberculosis* infection remains uncertain. Our model predicts that during latency lymphocyte populations at the site of infection are mainly of Th0 type, with very low levels of effector T cells (Th1 and Th2). This might explain the Th1/Th2 controversy: since Th0 cells produce both Type I and Type II cytokines, the relative predominance of either Th1 or Th2 is actually due to the particular stage of Th0 cells at the time of experimental measures. Moreover, what T helper cell populations (Th1 or Th2) predominate during active TB could be affected by large degrees of freedom and uncertainty in data collecting: experimental measurements (PBMC and BAL samples) and timing of collection of these measures (how long after first infection we take the sample) could partially explain these conflicting results. Our model also predicts that during peak infection, comparing latency to primary TB, a faster migration of Th precursor cells from the DLNs to the lung may explain the host ability to contain bacteria in the latency outcome.

In our virtual latent infection scenario, the majority of bacteria are intracellular and levels of extracellular bacteria are below the level of detection of current assays. This confirms experimental results where no bacteria were found in the lung of latently infected mice and in non-human primates (Capuano et al., 2003). However a key open question is where the bacteria reside during latency. Our model predicts where the remaining bacteria are in latency: housed within MDCs and infected macrophages.

We also show how potential new treatment strategies could be implemented. Our model predicts that there are key processes in the system that if affected by treatment induce a latency result from an active disease state. These processes are key targets for therapeutic study.

Acknowledgements

The authors from Department of Microbiology and Immunology at the University of Michigan Medical School have been supported by grants from NIH (R01HL68526) and from the Biomedical Research Council University of Michigan Medical School.

Appendix

List of parameters (We use cells/ml, assuming $1\,cm^3 = 1$ ml, and pg/ml $\times$ 10^6 cells.) (Table 4).

Parameter estimation

A complete and detailed analysis of how parameters were estimated in the lung model can be found in (Wigginton and Kirschner, 2001). In building the lung-lymph node model presented here, the most difficult task was to estimate parameter values for rates within the lymph node, particularly for DCs.

Both DCs and macrophages are derived from the same cell lines, namely monocytes. Thus, based on the cell biology, a reasonable assumption was to use macrophage rates to account for a similar effect for DCs. For example, the rate of migration to the lymph node of immature DC induced by extracellular bacteria

[7] Simeone Marino, Joanne L. Flynn, Denise E. Kirschner (submitted October 2003), Dendritic Cell Trafficking And Antigen Presentation In The Human Immune Response To *Mycobacterium tuberculosis*.

[8] S. Ganguli et al. (submitted September 2003), Metapopulation model of granuloma formation in the lung during *Mycobacterium tuberculosis* infection.

[9] Jose L. Segovia-Juarez, Suman Ganguli, Denise E. Kirschner (to be submitted), An Agent Base Model of Granuloma Formation in *Mycobacterium tuberculosis* infection.

(δ_{10}) is based on the rate of infection of resting macrophages (k_2), since both processes are induced by extracellular bacteria. Thus, we used similar ranges in our simulations. The same reasoning is valid for the rate of recruitment of immature DCs at the site of infection induced by extracellular bacteria (δ_8). Its value was based on the parameter for maximal recruitment of resting macrophages induced by infected and activated macrophages (α_4). Immature DC half-life is set to the range of resting macrophages resting half-life term. As in all cases, a large range is allowed to test for uncertainty using the LHS method.

Table 4

Name	Latency	Range	Reference	Definition	Units
Macrophages					
s_M	5000	(3300–7000)	Estimated	M_R recruitment	M_R/ml day
α_4	0.04	(0.03–0.05)	Estimated	M_R recruitment induced by M_A and M_I	1/day
w	0.14	0.14	Estimated	weight	Scalar
k_4	0.36	(0.36–0.4)	(Rojas et al., 1999)	Max rate of M_A deactivation	1/day
sc_8	100	(100–500)	(Rojas et al., 1999)	Half-sat, IL-10 on M_A deactivation	pg/ml
k_2	0.4	(0.2–0.4)	Estimated	Max M_R chronic infection induced by B_E	1/day
c_9	1E6	(1E6–1E7)	Estimated	Half-sat of M_R infection induced by B_E	B_E/ml
k_3	0.4	(0.2–0.4)	Estimated	Max M_R activation	1/day
f_3	2.333	(2–410)	(Zhang et al., 1995)	Adjustment, IFN-γ/IL-4 on M_A	Scalar
sc_3	150	(50–150)	Estimated	Half-sat, IFN-γ on M_R activation	pg/ml
c_8	5E5	(5E4–5E5)	(Flesch and Kaufmann, 1990)	Half-sat, B_T on M_R activation	B_T/ml
μ_R	0.01	0.011	(Van Furth et al., 1973)	Half-life of M_R	1/day
μ_A	0.01	0.011	(Van Furth et al., 1973)	Half-life of M_A	1/day
k_{17}	0.1	(0.05–0.5)	(Rojas et al., 1997)	Max M_I death due to bacteria	1/day
m	2	2	Estimated	Hill exponent	Scalar
k_{14}	0.5	(0.7–2)	(Lewinsohn et al., 1998; Tan et al., 1997; Tsukaguchi et al., 1995; Silver et al., 1998a, b)	Maximal T cell killing of M_I	1/day
c_4	0.15	(0.05–1)	(Oddo et al., 1998; Tsukaguchi et al., 1995; Silver et al., 1998a, b)	Half-sat, Th1 to M_I ratio for M_I lysis	T_1/M_I
μ_I	0.01	0.01	(Van Furth et al., 1973)	Half-life of M_I	1/day
Cytokines					
α_8	0.0008	0.0008	(Chensue et al., 1995; Zhang et al., 1994, 1995)	IL-12 production by M_A	(pg/M_A) day
α_{23}	2.75E-06	(2.75E-7–2.75E-4)	(Chensue et al., 1995; Fulton et al., 1998; Zhang et al., 1994)	IL-12 production by M_R (induced by B_T)	(pg/M_R) day
$\mu_{I_{12}^L}$	1.188	1.188	(Remick and Friedland, 1997)	Half-life of IL-12	1/day
s_g	700	(360–730)	(Tsukaguchi et al., 1995, 1999; Westermann and Pabst, 1992)	IFN-γ production by other sources (NK, CD8, etc.)	(pg/ml) day
c_{10}	5E3	(1E3–5E4)	(Fulton et al., 1996)	Half-sat, B_T on extra IFN-γ production	B_T/ml
sc_4	50	(5–100)	(O'Donnell et al., 1999; D'Andrea et al., 1993)	Half-sat, IL-12 on extra IFN-γ production	pg/ml
α_5	0.02	(0.02–0.066)	(Barnes et al., 1993; Fulton et al., 1998; Tsukaguchi et al., 1999)	IFN-γ production by Th1	(pg/T_1) day
c_5	1E5	(1E4–1E5)	Estimated	Half-sat, M_A on IFN-γ production of Th1 cells	M_A/ml
μ_g	3	(2.16–33.27)	(Kurzrock et al., 1985)	Half-life of IFN-γ	1/day
α_{14}	6E-3	(1.1E-3–1.1E-2)	(Tsukaguchi et al., 1999; Fulton et al., 1998; Isler et al., 1999)	Max rate of IL-10 production by M_A	(pg/M_A) day
sc_6	51	(51–58)	Estimated (Chomarat et al., 1993)	Half-sat, IL-10 and IFN-γ on IL-10	pg/ml
f_6	0.05	(0.025–0.053)	(Isler et al., 1999; Zhang et al., 1995; Chomarat et al., 1993)	Adjustment, IFN-γ/IL-10 on M_A production of IL-10	Scalar
α_{16}	5E-5	(5E-5–1E-3)	(Meyaard et al., 1996; Yssel et al., 1992)	IL-10 production by Th1	(pg/T_1) day

Table 4 (*continued*)

Name	Latency	Range	Reference	Definition	Units
α_{17}	1E-4	(1E-4–6E-3)	(Meyaard et al., 1996; Yssel et al., 1992)	IL-10 production by Th2	(pg/T_2) day
α_{18}	1E-4	(1E-4–6E-3)	(Meyaard et al., 1996; Yssel et al., 1992)	Max rate of IL-10 production by Th_P, induced by IL-12	(pg/T_P) day
δ_7	1E-4	1E-4	(Giacomini et al., 2001)	IL-10 production by M_I	(pg/M_I)/day
$\mu_{I_{10}}$	3.6968	(3.6968–7.23)	(Huhn et al., 1996, 1997)	Half-life of IL-10	1/day
α_{11}	0.0029	(2.8E-3–9.12E-3)	(Tsukaguchi et al., 1995)	IL-4 production by Th_P	(pg/T_P) day
α_{12}	0.0218	(2.8E-2–9.12E-2)	(Tsukaguchi et al., 1995)	IL-4 production by Th2	(pg/T_2) day
μ_{I_4}	2.77	2.77	(Remick and Friedland, 1997)	Half-life of IL-4	1/day
T cells					
δ_6	1.5E4	(1E3–1E5)	Estimated	Half-sat, M_A on Th_P migration	M_A/ml
α_2	4E-1	(1.4E-3–2.8)	(Janeway, 2001)	Max rate of Th_P proliferation induced by M_A	1/day
c_{15}	1E5	(1E4–1E5)	Estimated	Half-sat, M_A on Th_P proliferation	M_A/ml
μ_{T_0}	0.3333	(0.0111–0.3333)	(Sprent and Basten, 1973)	Half-life of Th_P	1/day
k_6	1E-01	(2.9E-4–1E-1)	(Sornasse et al., 1996; Assenmacher et al., 1998)	Rate of Th1 differentiation	(ml/pg) day
f_1	4.1	(2.9–410)	(Zhang et al., 1995)	Adjustment, IFN-γ + $IL\text{-}12_{LN}$/IL-4 on Th1 differentiation	Scalar
f_7	4.8	(4.8–65)	Estimated	Adjustment, IFN-γ + $IL\text{-}12_{LN}$/IL-10 on Th1 differentiation	Scalar
sc_1	30	(50–110)	Estimated	Half-sat, IFN-γ + $IL\text{-}12_{LN}$ on Th1 differentiation of Th_P	pg/ml
k_7	0.05	(0.02–0.7)	(Sornasse et al., 1996; Assenmacher et al., 1998)	Rate of Th2 differentiation	1/day
f_2	0.12	(0.0012–0.16)	(Zhang et al., 1995)	Adjustment, IL-4/IFN-γ on Th2 differentiation	Scalar
sc_2	2	(1–2)	Estimated	Half-sat, IL-4 on Th2 differentiation of Th_P	pg/ml
μ_{T_1}	0.3333	0.3333	(Sprent and Basten, 1973)	Half-life of Th1	1/day
μ_{T_2}	0.3333	0.3333	(Sprent and Basten, 1973)	Half-life of Th2	1/day
Bacteria					
α_{20}	0.005	(0–0.2591)	(Silver et al., 1998a, b; North and Izzo, 1993)	Growth rate of B_E	1/day
k_{15}	1.25E-07	1.25E-07	(Flesch and Kaufmann, 1990)	Max killing of B_E by M_A	(ml/M_A) day
k_{18}	1.25E-08	(1.25E-9–1.25E-8)	(Flesch and Kaufmann, 1990)	Max killing of B_E by M_R	(ml/M_R) day
α_{19}	0.1	(0.1–0.594)	(Silver et al., 1998a, b; Manca et al., 1999; Paul et al., 1996; Zhang et al., 1999)	Growth rate, intracellular bacteria	1/day
N	50	(50–100)	(Zhang et al., 1998; Paul et al., 1996; Hirsch et al., 1994)	Max MOI of M_I	B_I/M_I
N_1	20	(20–30)	Estimated	Max number of bacteria released after apoptosis	T_1/M_I
IL-12 in the DLN					
$\delta 1$	0.0035	(18E-4–65E-3)	(Giacomini et al., 2001)	IL-12 by MDC	(pg/MDC)/day
$\mu_{I_{12}^{LN}}$	1.188	1.188	(Remick and Friedland, 1997)	Half-life of IL-12	1/day
T cells in the DLN					
s_T	1000	1000	Estimated	Baseline Naïve *T*s circulating through the DLN	(T/ml)/day
δ_2	0.1	0.1	Estimated	Max recruitment of Naïve T cells to the DLN, induced by MDC	(T/MDC)/day
λ_1	0.1	0.1	Estimated	Recirculation rate of T cells through the DLN	1/day
μ_T	0.002	0.002	Estimated	Death rate of T cells	1/day
δ_4	0.0001	(1E-7–1E-1)	Estimated	Max T cell activation (from naïve to Th_P) by MDC	1/(day MDC)

Table 4 (*continued*)

Name	Latency	Range	Reference	Definition	Units
δ_5	0.9	(0.1–0.9)	Estimated	Half-sat, of Th_P in the DLN	1/day
ρ	3E3	(3E3–3E5)	Estimated	Threshold in Th_P proliferation	T/day
ξ	0.9	(0.3–0.95)	Estimated	% of Th_P migrating from the DLN to the Lung	1/day
φ	1	(1–15)	Estimated	Scaling factor	Scalar
Dendritic cells					
μ_{MDC}	0.02	0.02	Estimated	Half-life of MDC	1/day
δ_{12}	1E-07	(1.5E-8–1.5E-4)	Estimated	Bacteria uptake rate by IDC	1/(day IDC)
s_{IDC}	500	500	Estimated	Baseline IDC in the Lung	$\frac{DC/ml}{day}$
δ_8	0.02	(0.01–0.07)	Estimated	Max IDC recruitment to the site of infection (due to B_E)	1/day
δ_9	1.5E5	(1.5E5–1.5E6)	Estimated	Half-sat, B_E on IDC recruitment	B_E/ml
δ_{10}	0.2	(0.2–0.4)	Estimated	Max rate of IDC activation/ migration/maturation	1/day
δ_{11}	1E4	(1E3–1E5)	Estimated	Half-sat, B_E on IDC activation/ migration/maturation	B_E/ml
μ_{IDC}	0.01	0.01	Estimated	Half-life of IDC	1/day

Another assumption was to base rates within the lymph node on rates occurring at the site of infection. For example, the IL-12 decay rate in the lymph node was set to the range of IL-12 decay rate in the lung, as was the death rate of Th precursor cells.

Logistic growth, accounting for Th precursor cells proliferation within the lymph node, was estimated assuming a threshold (ρ) of 10^5 cells (reasonable considering the high turnover and migration rate of lymphocyte population within the draining lymph node) (Young and Hay, 1999; Young, 1999).

One critical parameter was δ_4, namely the maximal T cell activation rate induced by mature DC presentation in the lymph node. No quantitative data are available, thus we assumed that one MDC can prime one naïve T cell. We then estimated the value of δ_4 in order to fulfill that condition during latency, where both naïve T cells and mature DCs are at their steady levels. Assuming only one mature DC is present in the lymph node during latency (basically no presentation is performed), we have approximately 10^4 naïve T cells circulating through the lymph node: thus we set δ_4 equal to 10^{-4}. We indeed allow δ_4 to vary (between 10^{-7} and 10^{-1}) in order to investigate different hypothesis in term of antigen presentation activity in the lymph node (see Table 3).

References

Abu-Amero, K., 2002. Tuberculosis information on the web. J. R. Soc. Health 122 (2), 82.

Allen, J.E., Maizels, R.M., 1997. Th1–Th2: reliable paradigm or dangerous dogma? Immunol. Today 18 (8), 387.

Annunziato, F., Galli, G., Cosmi, L., Romagnani, P., Manetti, R., Maggi, E., Romagnani, S., 1998. Molecules associated with human Th1 or Th2 cells. Eur. Cytokine Network 9 (3 Suppl), 12.

Antony, V.B., Godbey, S.W., Kunkel, S.L., Hott, J.W., Hartman, D.L., Burdick, M.D., Strieter, R.M., 1993. Recruitment of inflammatory cells to the pleural space. Chemotactic cytokines, IL-8, and monocyte chemotactic peptide-1 in human pleural fluids. J. Immunol. 151 (12), 7216.

Appelberg, R., Orme, I.M., Pinto de Sousa, M.I., Silva, M.T., 1992. In vitro effects of interleukin-4 on interferon-gamma-induced macrophage activation. Immunology 76 (4), 553.

Arend, S.M., van Dissel, J.T., 2002. Evidence of endogenous reactivation of tuberculosis after a long period of latency. J. Infect. Dis. 186 (6), 876.

Assenmacher, M., Lohning, M., Scheffold, A., Richter, A., Miltenyi, S., Schmitz, J., Radbruch, A., 1998. Commitment of individual Th1-like lymphocytes to expression of IFN-gamma versus IL-4 and IL-10: selective induction of IL-10 by sequential stimulation of naive Th cells with IL-12 and IL-4. J. Immunol. 161 (6), 2825.

Balcewicz-Sablinska, M.K., Keane, J., Kornfeld, H., Remold, H.G., 1998. Pathogenic *Mycobacterium tuberculosis* evades apoptosis of host macrophages by release of TNF-R2, resulting in inactivation of TNF-alpha. J. Immunol. 161 (5), 2636.

Banchereau, J., Steinman, R.M., 1998. Dendritic cells and the control of immunity. Nature 392 (6673), 245.

Banchereau, J., Briere, F., Caux, C., Davoust, J., Lebecque, S., Liu, Y.J., Pulendran, B., Palucka, K., 2000. Immunobiology of dendritic cells. Annu. Rev. Immunol. 18, 767.

Barnes, P.F., Lu, S., Abrams, J.S., Wang, E., Yamamura, M., Modlin, R.L., 1993. Cytokine production at the site of disease in human tuberculosis. Infect. Immun. 61 (8), 3482.

Bellamy, R., Ruwende, C., Corrah, T., McAdam, K.P., Whittle, H.C., Hill, A.V., 1998. Variations in the NRAMP1 gene and susceptibility to tuberculosis in West Africans. N. Engl. J. Med. 338 (10), 640.

Bellamy, R., Ruwende, C., Corrah, T., McAdam, K.P., Thursz, M., Whittle, H.C., Hill, A.V., 1999. Tuberculosis and chronic hepatitis B virus infection in Africans and variation in the vitamin D receptor gene. J. Infect. Dis. 179 (3), 721.

Bhattacharyya, S., Singla, R., Dey, A.B., Prasad, H.K., 1999. Dichotomy of cytokine profiles in patients and high-risk healthy subjects exposed to tuberculosis. Infect. Immun. 67 (11), 5597.

Bloom, B.R., 1994. Tuberculosis: Pathogenesis, Protection, and Control. ASM Press, Washington, DC.

Blower, S.M., Dowlatabadi, H., 1994. Sensitivity and uncertainty analysis of complex-models of disease transmission—an HIV model, as an example. Int. Stat. Rev. 62 (2), 229.

Bodnar, K.A., Serbina, N.V., Flynn, J.L., 2001. Fate of *Mycobacterium tuberculosis* within murine dendritic cells. Infect. Immun. 69 (2), 800.

Bottomly, K., 1999. T cells and dendritic cells get intimate. Science 283 (5405), 1124.

Capuano III, S.V., Croix, D.A., Pawar, S., Zinovik, A., Myers, A., Lin, P.L., Bissel, S., Fuhrman, C., Klein, E., Flynn, J.L., 2003. Experimental *Mycobacterium tuberculosis* infection of cynomolgus macaques closely resembles the various manifestations of human M. tuberculosis infection. Infect. Immun. 71, 5831–5844.

Caruso, A.M., Serbina, N., Klein, E., Triebold, K., Bloom, B.R., Flynn, J.L., 1999. Mice deficient in CD4 T cells have only transiently diminished levels of IFN-gamma, yet succumb to tuberculosis. J. Immunol. 162 (9), 5407.

Chensue, S.W., Ruth, J.H., Warmington, K., Lincoln, P., Kunkel, S.L., 1995. In vivo regulation of macrophage IL-12 production during type 1 and type 2 cytokine-mediated granuloma formation. J. Immunol. 155 (7), 3546.

Choi, M.S., Lee, J.H., Koh, K.C., Paik, S.W., Rhee, P.L., Kim, J.J., Rhee, J.C., Choi, K.W., Kim, S.H., 2001. Clinical significance of enlarged perihepatic lymph nodes in chronic hepatitis B. J. Clin. Gastroenterol. 32 (4), 329.

Chomarat, P., Rissoan, M.C., Banchereau, J., Miossec, P., 1993. Interferon gamma inhibits interleukin 10 production by monocytes. J. Exp. Med. 177 (2), 523.

Comstock, G.W., Livesay, V.T., Woolpert, S.F., 1974. The prognosis of a positive tuberculin reaction in childhood and adolescence. Am. J. Epidemiol. 99 (2), 131.

Condos, R., Rom, W.N., Liu, Y.M., Schluger, N.W., 1998. Local immune responses correlate with presentation and outcome in tuberculosis. Am. J. Respir. Crit. Care. Med. 157 (3 Pt 1), 729.

Cooper, A.M., Dalton, D.K., Stewart, T.A., Griffin, J.P., Russell, D.G., Orme, I.M., 1993. Disseminated tuberculosis in interferon gamma gene-disrupted mice. J. Exp. Med. 178 (6), 2243.

Cooper, A.M., Magram, J., Ferrante, J., Orme, I.M., 1997. Interleukin 12 (IL-12) is crucial to the development of protective immunity in mice intravenously infected with *Mycobacterium tuberculosis*. J. Exp. Med. 186 (1), 39.

Crowle, A.J., Elkins, N., 1990. Relative permissiveness of macrophages from black and white people for virulent tubercle bacilli. Infect. Immun. 58 (3), 632.

D'Andrea, A., Aste-Amezaga, M., Valiante, N.M., Ma, X., Kubin, M., Trinchieri, G., 1993. Interleukin 10 (IL-10) inhibits human lymphocyte interferon gamma-production by suppressing natural killer cell stimulatory factor/IL-12 synthesis in accessory cells. J. Exp. Med. 178 (3), 1041.

Demangel, C., Britton, W.J., 2000. Interaction of dendritic cells with mycobacteria: where the action starts. Immunol. Cell Biol. 78 (4), 318.

DesJardin, L.E., Kaufman, T.M., Potts, B., Kutzbach, B., Yi, H., Schlesinger, L.S., 2002. *Mycobacterium tuberculosis*-infected human macrophages exhibit enhanced cellular adhesion with increased expression of LFA-1 and ICAM-1 and reduced expression and/or function of complement receptors, FcgammaRII and the mannose receptor. Microbiology 148 (Pt 10), 3161.

de Waal Malefyt, R., Figdor, C.G., de Vries, J.E., 1993. Effects of interleukin 4 on monocyte functions: comparison to interleukin 13. Res. Immunol. 144 (8), 629.

Dlugovitzky, D., Bay, M.L., Rateni, L., Urizar, L., Rondelli, C.F., Largacha, C., Farroni, M.A., Molteni, O., Bottasso, O.A., 1999. In vitro synthesis of interferon-gamma, interleukin-4, transforming growth factor-beta and interleukin-1 beta by peripheral blood mononuclear cells from tuberculosis patients: relationship with the severity of pulmonary involvement. Scand. J. Immunol. 49 (2), 210.

Dye, C., Scheele, S., Dolin, P., Pathania, V., Raviglione, M.C., 1999. Consensus statement. Global burden of tuberculosis: estimated incidence, prevalence, and mortality by country. WHO Global Surveillance and Monitoring Project. J. Am. Med. Assoc. 282 (7), 677.

Feng, C.G., Demangel, C., Kamath, A.T., Macdonald, M., Britton, W.J., 2001. Dendritic cells infected with Mycobacterium bovis bacillus Calmette Guerin activate CD8(+) T cells with specificity for a novel mycobacterial epitope. Int. Immunol. 13 (4), 451.

Fenhalls, G., Stevens, L., Moses, L., Bezuidenhout, J., Betts, J.C., Helden, Pv.P., Lukey, P.T., Duncan, K., 2002. In situ detection of *Mycobacterium tuberculosis* transcripts in human lung granulomas reveals differential gene expression in necrotic lesions. Infect. Immun. 70 (11), 6330.

Flesch, I.E., Kaufmann, S.H., 1990. Activation of tuberculostatic macrophage functions by gamma interferon, interleukin-4, and tumor necrosis factor. Infect. Immun. 58 (8), 2675.

Flynn, J.L., Chan, J., 2001. Immunology of tuberculosis. Annu. Rev. Immunol. 19, 93.

Flynn, J.L., Chan, J., Triebold, K.J., Dalton, D.K., Stewart, T.A., Bloom, B.R., 1993. An essential role for interferon gamma in resistance to *Mycobacterium tuberculosis* infection. J. Exp. Med. 178 (6), 2249.

Fortsch, D., Rollinghoff, M., Stenger, S., 2000. IL-10 converts human dendritic cells into macrophage-like cells with increased antibacterial activity against virulent *Mycobacterium tuberculosis*. J. Immunol. 165 (2), 978.

Fulton, S.A., Johnsen, J.M., Wolf, S.F., Sieburth, D.S., Boom, W.H., 1996. Interleukin-12 production by human monocytes infected with *Mycobacterium tuberculosis*: role of phagocytosis. Infect. Immun. 64 (7), 2523.

Fulton, S.A., Cross, J.V., Toossi, Z.T., Boom, W.H., 1998. Regulation of interleukin-12 by interleukin-10, transforming growth factor-beta, tumor necrosis factor-alpha, and interferon-gamma in human monocytes infected with *Mycobacterium tuberculosis* H37Ra. J. Infect. Dis. 178 (4), 1105.

Gammack, D., C.R. Doering and D.E. Kirschner, 2003. Macrophage response to *Mycobacterium tuberculosis* infection, J. Math. Biol. Published online: 20 August 2003, (to appear) Feb 2004.

Giacomini, E., Iona, E., Ferroni, L., Miettinen, M., Fattorini, L., Orefici, G., Julkunen, I., Coccia, E.M., 2001. Infection of human macrophages and dendritic cells with *Mycobacterium tuberculosis* induces a differential cytokine gene expression that modulates T cell response. J. Immunol. 166 (12), 7033.

Gonzalez-Juarrero, M., Orme, I.M., 2001. Characterization of murine lung dendritic cells infected with *Mycobacterium tuberculosis*. Infect. Immun. 69 (2), 1127.

Greenland, S., 2001. Sensitivity analysis, Monte Carlo risk analysis, and Bayesian uncertainty assessment. Risk. Anal. 21 (4), 579.

Guermonprez, P., Valladeau, J., Zitvogel, L., Thery, C., Amigorena, S., 2002. Antigen presentation and T cell stimulation by dendritic cells. Annu. Rev. Immunol. 20, 621.

Havenith, C.E., Breedijk, A.J., Hoefsmit, E.C., 1992. Effect of bacillus Calmette-Guerin inoculation on numbers of dendritic cells in bronchoalveolar lavages of rats. Immunobiology 184 (4–5), 336.

Helton, J.C., Davis, F.J., 2002. Illustration of sampling-based methods for uncertainty and sensitivity analysis. Risk Anal. 22 (3), 591.

Henderson, R.A., Watkins, S.C., Flynn, J.L., 1997. Activation of human dendritic cells following infection with *Mycobacterium tuberculosis*. J. Immunol. 159 (2), 635.

Hernandez-Pando, R., Rook, G.A., 1994. The role of TNF-alpha in T-cell-mediated inflammation depends on the Th1/Th2 cytokine balance. Immunology 82 (4), 591.

Hickman, S.P., Chan, J., Salgame, P., 2002. *Mycobacterium tuberculosis* induces differential cytokine production from dendritic cells and macrophages with divergent effects on naive T cell polarization. J. Immunol. 168 (9), 4636.

Hirsch, C.S., Yoneda, T., Averill, L., Ellner, J.J., Toossi, Z., 1994. Enhancement of intracellular growth of *Mycobacterium tuberculosis* in human monocytes by transforming growth factor-beta 1. J. Infect. Dis. 170 (5), 1229.

Holt, P.G., 2000. Antigen presentation in the lung. Am. J. Respir. Crit. Care Med. 162 (4 Pt 2), S151. #6.

Holt, P.G., Schon-Hegrad, M.A., 1987. Localization of T cells, macrophages and dendritic cells in rat respiratory tract tissue: implications for immune function studies. Immunology 62 (3), 349.

Holt, P.G., Stumbles, P.A., 2000a. Characterization of dendritic cell populations in the respiratory tract. J. Aerosol. Med. 13 (4), 361. #8.

Holt, P.G., Stumbles, P.A., 2000b. Regulation of immunologic homeostasis in peripheral tissues by dendritic cells: the respiratory tract as a paradigm. J. Allergy Clin. Immunol. 105 (3), 421. #9.

Holt, P.G., Oliver, J., Bilyk, N., McMenamin, C., McMenamin, P.G., Kraal, G., Thepen, T., 1993. Downregulation of the antigen presenting cell function(s) of pulmonary dendritic cells in vivo by resident alveolar macrophages. J. Exp. Med. 177 (2), 397.

Huhn, R.D., Radwanski, E., O'Connell, S.M., Sturgill, M.G., Clarke, L., Cody, R.P., Affrime, M.B., Cutler, D.L., 1996. Pharmacokinetics and immunomodulatory properties of intravenously administered recombinant human interleukin-10 in healthy volunteers. Blood 87 (2), 699.

Huhn, R.D., Radwanski, E., Gallo, J., Affrime, M.B., Sabo, R., Gonyo, G., Monge, A., Cutler, D.L., 1997. Pharmacodynamics of subcutaneous recombinant human interleukin-10 in healthy volunteers. Clin. Pharmacol. Ther. 62 (2), 171.

Iseman, M.D., 1999a. International Union against Tuberculosis and Lung Disease. World Conference. Update treatment of multidrug-resistant tuberculosis: Proceedings of a sponsored symposium to the 29th World Conference of the International Union against Tuberculosis and Lung Diseases (IUATLD/UICTMR), Bangkok, Thailand, November 24, 1998. S. Karger, Basel, New York.

Iseman, M.D., 1999b. Treatment and implications of multidrug-resistant tuberculosis for the 21st century. Chemotherapy 45, 34–40.

Iseman, M.D., 2002. Tuberculosis therapy: past, present and future. Eur. Respir. J. Suppl. 36, 87s–94s.

Isler, P., de Rochemonteix, B.G., Songeon, F., Boehringer, N., Nicod, L.P., 1999. Interleukin-12 production by human alveolar macrophages is controlled by the autocrine production of interleukin-10. Am. J. Respir. Cell. Mol. Biol. 20 (2), 270.

Janeway, C., 2001. Immunobiology 5: The Immune System in Health and Disease. Garland Pub., New York. #201.

Jiao, X., Lo-Man, R., Guermonprez, P., Fiette, L., Deriaud, E., Burgaud, S., Gicquel, B., Winter, N., Leclerc, C., 2002. Dendritic cells are host cells for mycobacteria in vivo that trigger innate and acquired immunity. J. Immunol. 168 (3), 1294.

Jung, Y.J., LaCourse, R., Ryan, L., North, R.J., 2002. Evidence inconsistent with a negative influence of T helper 2 cells on protection afforded by a dominant T helper 1 response against *Mycobacterium tuberculosis* lung infection in mice. Infect. Immun. 70 (11), 6436.

Keane, J., Remold, H.G., Kornfeld, H., 2000. Virulent *Mycobacterium tuberculosis* strains evade apoptosis of infected alveolar macrophages. J. Immunol. 164 (4), 2016.

Kirschner, D., 1999. Dynamics of co-infection with M. Tuberculosis and HIV-1. Theor. Popul. Biol. 55, 94–109.

Klopfens, Rw., 1971. Numerical Differentiation Formulas for Stiff Systems of Ordinary Differential Equations. Rca Rev. 32 (3), 447.

Kurzrock, R., Rosenblum, M.G., Sherwin, S.A., Rios, A., Talpaz, M., Quesada, J.R., Gutterman, J.U., 1985. Pharmacokinetics, single-dose tolerance, and biological activity of recombinant gamma-interferon in cancer patients. Cancer Res. 45 (6), 2866.

Lai, C.K., Ho, S., Chan, C.H., Chan, J., Choy, D., Leung, R., Lai, K.N., 1997. Cytokine gene expression profile of circulating CD4+ T cells in active pulmonary tuberculosis. Chest 111 (3), 606.

Lalvani, A., Brookes, R., Wilkinson, R.J., Malin, A.S., Pathan, A.A., Andersen, P., Dockrell, H., Pasvol, G., Hill, A.V., 1998. Human cytolytic and interferon gamma-secreting CD8+ T lymphocytes specific for *Mycobacterium tuberculosis*. Proc. Natl Acad. Sci. USA 95 (1), 270.

Langenkamp, A., Messi, M., Lanzavecchia, A., Sallusto, F., 2000. Kinetics of dendritic cell activation: impact on priming of TH1, TH2 and nonpolarized T cells. Nat. Immunol. 1 (4), 311.

Langermans, J.A., Andersen, P., van Soolingen, D., Vervenne, R.A., Frost, P.A., van der Laan, T., van Pinxteren, L.A., van den Hombergh, J., Kroon, S., Peekel, I., Florquin, S., Thomas, A.W., 2001. Divergent effect of bacillus Calmette-Guerin (BCG) vaccination on *Mycobacterium tuberculosis* infection in highly related macaque species: implications for primate models in tuberculosis vaccine research. Proc. Natl Acad. Sci. USA 98 (20), 11497.

Lanzavecchia, A., Sallusto, F., 2000. Dynamics of T lymphocyte responses: intermediates, effectors, and memory cells. Science 290 (5489), 92.

Lanzavecchia, A., Sallusto, F., 2001a. The instructive role of dendritic cells on T cell responses: lineages, plasticity and kinetics. Curr. Opin. Immunol. 13 (3), 291. #122.

Lanzavecchia, A., Sallusto, F., 2001b. Regulation of T cell immunity by dendritic cells. Cell 106 (3), 263. #123.

Law, K., Weiden, M., Harkin, T., Tchou-Wong, K., Chi, C., Rom, W.N., 1996. Increased release of interleukin-1 beta, interleukin-6, and tumor necrosis factor-alpha by bronchoalveolar cells lavaged from involved sites in pulmonary tuberculosis. Am. J. Respir. Crit. Care Med. 153 (2), 799.

Lazarevic, V., Flynn, J., 2002. CD8(+) T cells in tuberculosis. Am. J. Respir. Crit. Care Med. 166 (8), 1116.

Lewinsohn, D.M., Bement, T.T., Xu, J., Lynch, D.H., Grabstein, K.H., Reed, S.G., Alderson, M.R., 1998. Human purified protein derivative-specific CD4+ T cells use both CD95-dependent and CD95-independent cytolytic mechanisms. J. Immunol. 160 (5), 2374.

Lillebaek, T., Dirksen, A., Baess, I., Strunge, B., Thomsen, V.O., Andersen, A.B., 2002. Molecular evidence of endogenous reactivation of *Mycobacterium tuberculosis* after 33 years of latent infection. J. Infect. Dis. 185 (3), 401.

Lin, Y., Zhang, M., Hofman, F.M., Gong, J., Barnes, P.F., 1996. Absence of a prominent Th2 cytokine response in human tuberculosis. Infect. Immun. 64 (4), 1351.

Lin, C.L., Sewell, A.K., Gao, G.F., Whelan, K.T., Phillips, R.E., Austyn, J.M., 2000. Macrophage-tropic HIV induces and exploits dendritic cell chemotaxis. J. Exp. Med. 192 (4), 587.

Lucey, D.R., Clerici, M., Shearer, G.M., 1996. Type 1 and type 2 cytokine dysregulation in human infectious, neoplastic, and inflammatory diseases. Clin. Microbiol. Rev. 9 (4), 532.

Maggi, E., Parronchi, P., Manetti, R., Simonelli, C., Piccinni, M.P., Rugiu, F.S., De Carli, M., Ricci, M., Romagnani, S., 1992. Reciprocal regulatory effects of IFN-gamma and IL-4 on the in vitro development of human Th1 and Th2 clones. J. Immunol. 148 (7), 2142.

Manca, C., Tsenova, L., Barry III, C.E., Bergtold, A., Freeman, S., Haslett, P.A., Musser, J.M., Freedman, V.H., Kaplan, G., 1999. *Mycobacterium tuberculosis* CDC1551 induces a more vigorous

host response in vivo and in vitro, but is not more virulent than other clinical isolates. J. Immunol. 162 (11), 6740.

Manetti, R., Parronchi, P., Giudizi, M.G., Piccinni, M.P., Maggi, E., Trinchieri, G., Romagnani, S., 1993. Natural killer cell stimulatory factor (interleukin 12 [IL-12]) induces T helper type 1 (Th1)-specific immune responses and inhibits the development of IL-4-producing Th cells. J. Exp. Med. 177 (4), 1199.

McDonough, K.A., Kress, Y., Bloom, B.R., 1993. Pathogenesis of tuberculosis: interaction of *Mycobacterium tuberculosis* with macrophages. Infect. Immun. 61 (7), 2763.

Mercer, R.R., Russell, M.L., Roggli, V.L., Crapo, J.D., 1994. Cell number and distribution in human and rat airways. Am. J. Respir. Cell Mol. Biol. 10 (6), 613.

Meyaard, L., Hovenkamp, E., Otto, S.A., Miedema, F., 1996. IL-12-induced IL-10 production by human T cells as a negative feedback for IL-12-induced immune responses. J. Immunol. 156 (8), 2776.

Moore, K.W., de Waal Malefyt, R., Coffman, R.L., O'Garra, A., 2001. Interleukin-10 and the interleukin-10 receptor. Annu. Rev. Immunol. 19, 683.

Nathan, C.F., Murray, H.W., Wiebe, M.E., Rubin, B.Y., 1983. Identification of interferon-gamma as the lymphokine that activates human macrophage oxidative metabolism and antimicrobial activity. J. Exp. Med. 158 (3), 670.

Newport, M.J., Huxley, C.M., Huston, S., Hawrylowicz, C.M., Oostra, B.A., Williamson, R., Levin, M., 1996. A mutation in the interferon-gamma-receptor gene and susceptibility to mycobacterial infection. N. Engl. J. Med. 335 (26), 1941.

North, R.J., 1998. Mice incapable of making IL-4 or IL-10 display normal resistance to infection with *Mycobacterium tuberculosis*. Clin. Exp. Immunol. 113 (1), 55.

North, R.J., Izzo, A.A., 1993. Mycobacterial virulence. Virulent strains of Mycobacteria tuberculosis have faster in vivo doubling times and are better equipped to resist growth-inhibiting functions of macrophages in the presence and absence of specific immunity. J. Exp. Med. 177 (6), 1723.

Oddo, M., Renno, T., Attinger, A., Bakker, T., MacDonald, H.R., Meylan, P.R., 1998. Fas ligand-induced apoptosis of infected human macrophages reduces the viability of intracellular *Mycobacterium tuberculosis*. J. Immunol. 160 (11), 5448.

O'Donnell, M.A., Luo, Y., Chen, X., Szilvasi, A., Hunter, S.E., Clinton, S.K., 1999. Role of IL-12 in the induction and potentiation of IFN-gamma in response to bacillus Calmette-Guerin. J. Immunol. 163 (8), 4246.

O'Garra, A., 1998. Cytokines induce the development of functionally heterogeneous T helper cell subsets. Immunity 8 (3), 275.

Palucka, K.A., Taquet, N., Sanchez-Chapuis, F., Gluckman, J.C., 1998. Dendritic cells as the terminal stage of monocyte differentiation. J. Immunol. 160 (9), 4587.

Paul, S., Laochumroonvorapong, P., Kaplan, G., 1996. Comparable growth of virulent and avirulent *Mycobacterium tuberculosis* in human macrophages in vitro. J. Infect. Dis. 174 (1), 105.

Peng, X., Kasran, A., Ceuppens, J.L., 1997. Interleukin 12 and B7/CD28 interaction synergistically upregulate interleukin 10 production by human T cells. Cytokine 9 (7), 499.

Powrie, F., Coffman, R.L., 1993. Inhibition of cell-mediated immunity by IL4 and IL10. Res. Immunol. 144 (8), 639.

Remick, D.G., Friedland, J.S., 1997. Cytokines in Health and Disease, 2nd Review and Expand Edition. Marcel Dekker, New York.

Rescigno, M., 2002. Dendritic cells and the complexity of microbial infection. Trends Microbiol. 10 (9), 425.

Rescigno, M., Borrow, P., 2001. The host–pathogen interaction: new themes from dendritic cell biology. Cell 106 (3), 267.

Rojas, M., Barrera, L.F., Puzo, G., Garcia, L.F., 1997. Differential induction of apoptosis by virulent *Mycobacterium tuberculosis* in resistant and susceptible murine macrophages: role of nitric oxide and mycobacterial products. J. Immunol. 159 (3), 1352.

Rojas, M., Olivier, M., Gros, P., Barrera, L.F., Garcia, L.F., 1999. TNF-alpha and IL-10 modulate the induction of apoptosis by virulent *Mycobacterium tuberculosis* in murine macrophages. J. Immunol. 162 (10), 6122.

Romagnani, S., 1998. The Th1/Th2 paradigm and allergic disorders. Allergy 53 (46), 12.

Romagnani, S., 1999. Th1/Th2 cells. Inflamm. Bowel Dis. 5 (4), 285.

Romagnani, S., 2000. T-cell subsets (Th1 versus Th2). Ann. Allergy Asthma Immunol. 85 (1), 9.

Romagnani, S., Kapsenberg, M., Radbruch, A., Adorini, L., 1998. Th1 and Th2 cells. Res. Immunol. 149 (9), 871.

Rook, G., 2001. Th1- or Th2-cell commitment during infectious disease: an oversimplification? Trends Immunol. 22 (9), 481.

Rosenbrock, H.H., Storey, C., 1970. Mathematics of Dynamical Systems. Wiley Interscience Division, New York.

Russo, D.M., Kozlova, N., Lakey, D.L., Kernodle, D., 2000. Naive human T cells develop into Th1 effectors after stimulation with *Mycobacterium tuberculosis*-infected macrophages or recombinant Ag85 proteins. Infect. Immun. 68 (12), 6826.

Sallusto, F., Lanzavecchia, A., 2000. Understanding dendritic cell and T-lymphocyte traffic through the analysis of chemokine receptor expression. Immunol. Rev. 177, 134.

Sallusto, F., Lanzavecchia, A., Mackay, C.R., 1998. Chemokines and chemokine receptors in T-cell priming and Th1/Th2-mediated responses. Immunol. Today 19 (12), 568.

Sallusto, F., Lenig, D., Forster, R., Lipp, M., Lanzavecchia, A., 1999. Two subsets of memory T lymphocytes with distinct homing potentials and effector functions. Nature 401 (6754), 708.

Sallusto, F., Mackay, C.R., Lanzavecchia, A., 2000. The role of chemokine receptors in primary, effector, and memory immune responses. Annu. Rev. Immunol. 18, 593.

Sanchez, M.A., Blower, S.M., 1997. Uncertainty and sensitivity analysis of the basic reproductive rate. Tuberculosis as an example. Am. J. Epidemiol. 145 (12), 1127.

Schwander, S.K., Torres, M., Sada, E., Carranza, C., Ramos, E., Tary-Lehmann, M., Wallis, R.S., Sierra, J., Rich, E.A., 1998. Enhanced responses to *Mycobacterium tuberculosis* antigens by human alveolar lymphocytes during active pulmonary tuberculosis. J. Infect. Dis. 178 (5), 1434.

Seah, G.T., Rook, G.A., 2001. Il-4 influences apoptosis of mycobacterium-reactive lymphocytes in the presence of TNF-alpha. J. Immunol. 167 (3), 1230.

Serbina, N.V., Flynn, J.L., 1999. Early emergence of CD8(+) T cells primed for production of type 1 cytokines in the lungs of *Mycobacterium tuberculosis*-infected mice. Infect. Immun. 67 (8), 3980.

Serbina, N.V., Flynn, J.L., 2001. CD8(+) T cells participate in the memory immune response to *Mycobacterium tuberculosis*. Infect. Immun. 69 (7), 4320.

Sertl, K., Takemura, T., Tschachler, E., Ferrans, V.J., Kaliner, M.A., Shevach, E.M., 1986. Dendritic cells with antigen-presenting capability reside in airway epithelium, lung parenchyma, and visceral pleura. J. Exp. Med. 163 (2), 436.

Silver, R.F., Li, Q., Ellner, J.J., 1998a. Expression of virulence of *Mycobacterium tuberculosis* within human monocytes: virulence correlates with intracellular growth and induction of tumor necrosis factor alpha but not with evasion of lymphocyte-dependent monocyte effector functions. Infect. Immun. 66 (3), 1190.

Silver, R.F., Li, Q., Boom, W.H., Ellner, J.J., 1998b. Lymphocyte-dependent inhibition of growth of virulent *Mycobacterium tuberculosis* H37Rv within human monocytes: requirement for CD4+T cells in purified protein derivative-positive, but not in purified protein derivative-negative subjects. J. Immunol. 160 (5), 2408.

Skinner, M.A., Yuan, S., Prestidge, R., Chuk, D., Watson, J.D., Tan, P.L., 1997. Immunization with heat-killed Mycobacterium vaccae stimulates CD8+ cytotoxic T cells specific for macrophages infected with *Mycobacterium tuberculosis*. Infect. Immun. 65 (11), 4525.

Sornasse, T., Larenas, P.V., Davis, K.A., de Vries, J.E., Yssel, H., 1996. Differentiation and stability of T helper 1 and 2 cells derived from naive human neonatal CD4+ T cells, analyzed at the single-cell level. J. Exp. Med. 184 (2), 473.

Sprent, J., Basten, A., 1973. Circulating T and B lymphocytes of the mouse. II. Lifespan. Cell Immunol. 7 (1), 40.

Stead, W.W., Senner, J.W., Reddick, W.T., Lofgren, J.P., 1990. Racial differences in susceptibility to infection by *Mycobacterium tuberculosis*. N. Engl. J. Med. 322 (7), 422.

Stone, K.C., Mercer, R.R., Gehr, P., Stockstill, B., Crapo, J.D., 1992. Allometric relationships of cell numbers and size in the mammalian lung. Am. J. Respir. Cell. Mol. Biol. 6 (2), 235.

Stout, R.D., Bottomly, K., 1989. Antigen-specific activation of effector macrophages by IFN-gamma producing (TH1) T cell clones. Failure of IL-4-producing (TH2) T cell clones to activate effector function in macrophages. J. Immunol. 142 (3), 760.

Sturgill-Koszycki, S., Schlesinger, P.H., Chakraborty, P., Haddix, P.L., Collins, H.L., Fok, A.K., Allen, R.D., Gluck, S.L., Heuser, J., Russell, D.G., 1994. Lack of acidification in Mycobacterium phagosomes produced by exclusion of the vesicular proton-ATPase. Science 263 (5147), 678.

Surcel, H.M., Troye-Blomberg, M., Paulie, S., Andersson, G., Moreno, C., Pasvol, G., Ivanyi, J., 1994. Th1/Th2 profiles in tuberculosis, based on the proliferation and cytokine response of blood lymphocytes to mycobacterial antigens. Immunology 81 (2), 171.

Szabo, S.J., Dighe, A.S., Gubler, U., Murphy, K.M., 1997. Regulation of the interleukin (IL)-12R beta 2 subunit expression in developing T helper 1 (Th1) and Th2 cells. J. Exp. Med. 185 (5), 817.

Tan, J.S., Canaday, D.H., Boom, W.H., Balaji, K.N., Schwander, S.K., Rich, E.A., 1997. Human alveolar T lymphocyte responses to *Mycobacterium tuberculosis* antigens: role for CD4+ and CD8+ cytotoxic T cells and relative resistance of alveolar macrophages to lysis. J. Immunol. 159 (1), 290.

Tascon, R.E., Stavropoulos, E., Lukacs, K.V., Colston, M.J., 1998. Protection against *Mycobacterium tuberculosis* infection by CD8+ T cells requires the production of gamma interferon. Infect. Immun. 66 (2), 830.

Tsukaguchi, K., Balaji, K.N., Boom, W.H., 1995. CD4+ alpha beta T cell and gamma delta T cell responses to *Mycobacterium tuberculosis*. Similarities and differences in Ag recognition, cytotoxic effector function, and cytokine production. J. Immunol. 154 (4), 1786.

Tsukaguchi, K., de Lange, B., Boom, W.H., 1999. Differential regulation of IFN-gamma, TNF-alpha, and IL-10 production by CD4(+) alphabeta TCR+ T cells and vdelta2(+) gammadelta T cells in response to monocytes infected with *Mycobacterium tuberculosis*-H37Ra. Cell Immunol. 194 (1), 12.

van Crevel, R., Karyadi, E., Preyers, F., Leenders, M., Kullberg, B.J., Nelwan, R.H., van der Meer, J.W., 2000. Increased production of interleukin 4 by CD4+ and CD8+ T cells from patients with tuberculosis is related to the presence of pulmonary cavities. J. Infect. Dis. 181 (3), 1194.

van Crevel, R., Ottenhoff, T.H., van der Meer, J.W., 2002. Innate immunity to *Mycobacterium tuberculosis*. Clin. Microbiol. Rev. 15 (2), 294.

Van Furth, R., Diesselhoff-den Dulk, M.C., Mattie, H., 1973. Quantitative study on the production and kinetics of mononuclear phagocytes during an acute inflammatory reaction. J. Exp. Med. 138 (6), 1314.

van Haarst, J.M., de Wit, H.J., Drexhage, H.A., Hoogsteden, H.C., 1994. Distribution and immunophenotype of mononuclear phagocytes and dendritic cells in the human lung. Am. J. Respir. Cell. Mol. Biol. 10 (5), 487.

von Andrian, U.H., Mackay, C.R., 2000. T-cell function and migration. Two sides of the same coin. N. Engl. J. Med. 343 (14), 1020.

Wakeham, J., Wang, J., Magram, J., Croitoru, K., Harkness, R., Dunn, P., Zganiacz, A., Xing, Z., 1998. Lack of both types 1 and 2 cytokines, tissue inflammatory responses, and immune protection during pulmonary infection by *Mycobacterium bovis* bacille Calmette-Guerin in IL-12-deficient mice. J. Immunol. 160 (12), 6101.

Westermann, J., Pabst, R., 1992. Distribution of lymphocyte subsets and natural killer cells in the human body. Clin. Invest. 70 (7), 539.

Wigginton, J.E., Kirschner, D., 2001. A model to predict cell-mediated immune regulatory mechanisms during human infection with *Mycobacterium tuberculosis*. J. Immunol. 166 (3), 1951.

Wilkinson, R.J., Patel, P., Llewelyn, M., Hirsch, C.S., Pasvol, G., Snounou, G., Davidson, R.N., Toossi, Z., 1999. Influence of polymorphism in the genes for the interleukin (IL)-1 receptor antagonist and IL-1beta on tuberculosis. J. Exp. Med. 189 (12), 1863.

Wilkinson, R.J., Llewelyn, M., Toossi, Z., Patel, P., Pasvol, G., Lalvani, A., Wright, D., Latif, M., Davidson, R.N., 2000. Influence of vitamin D deficiency and vitamin D receptor polymorphisms on tuberculosis among Gujarati Asians in west London: a case-control study. Lancet 355 (9204), 618.

Young, A.J., 1999. The physiology of lymphocyte migration through the single lymph node in vivo. Semin. Immunol. 11 (2), 73.

Young, A.J., Hay, J., 1999. Lymphocyte migration in development and disease. Semin. Immunol. 11 (2), 71.

Yssel, H., De Waal Malefyt, R., Roncarolo, M.G., Abrams, J.S., Lahesmaa, R., Spits, H., de Vries, J.E., 1992. IL-10 is produced by subsets of human CD4+ T cell clones and peripheral blood T cells. J. Immunol. 149 (7), 2378.

Zhang, M., Gately, M.K., Wang, E., Gong, J., Wolf, S.F., Lu, S., Modlin, R.L., Barnes, P.F., 1994. Interleukin 12 at the site of disease in tuberculosis. J. Clin. Invest. 93 (4), 1733.

Zhang, M., Lin, Y., Iyer, D.V., Gong, J., Abrams, J.S., Barnes, P.F., 1995. T-cell cytokine responses in human infection with *Mycobacterium tuberculosis*. Infect. Immun. 63 (8), 3231.

Zhang, M., Gong, J., Lin, Y., Barnes, P.F., 1998. Growth of virulent and avirulent *Mycobacterium tuberculosis* strains in human macrophages. Infect. Immun. 66 (2), 794.

Zhang, M., Gong, J., Yang, Z., Samten, B., Cave, M.D., Barnes, P.F., 1999. Enhanced capacity of a widespread strain of *Mycobacterium tuberculosis* to grow in human macrophages. J. Infect. Dis. 179 (5), 1213.

Zhu, K., Shen, Q., Ulrich, M., Zheng, M., 2000. Human monocyte-derived dendritic cells expressing both chemotactic cytokines IL-8, MCP-1, RANTES and their receptors, and their selective migration to these chemokines. Chin. Med. J. (Engl) 113 (12), 1124.